GAUGE THEORY AMPLITUDES, SCALAR GRAPHS AND TWISTOR SPACE

VALENTIN V. KHOZE

Department of Physics and IPPP
University of Durham
Durham, DH1 3LE
United Kingdom

We discuss a remarkable new approach initiated by Cachazo, Svrcek and Witten for calculating gauge theory amplitudes. The formalism amounts to an effective scalar perturbation theory which in many cases offers a much simpler alternative to the usual Feynman diagrams for deriving n-point amplitudes in gauge theory. At tree level the formalism works in a generic gauge theory, with or without supersymmetry, and for a finite number of colors. There is also growing evidence that the formalism works for loop amplitudes.

Table of Contents

1. Introduction

In a recent paper [1] Cachazo, Svrcek and Witten (CSW) proposed a new approach for calculating scattering amplitudes of n gluons. In this approach tree amplitudes in gauge theory are found by summing tree-level scalar diagrams. The CSW formalism [1] is constructed in terms of scalar propagators, $1/q^2$, and tree-level maximal helicity violating (MHV) amplitudes, which are interpreted as new scalar vertices. The MHV vertices already contain an arbitrary number of gluon lines, and are known explicitly [2,3]. Using multiparticle MHV amplitudes as effective vertices in a new perturbation theory enables one to save dramatically on the number of permutations found in usual Feynman diagrams.

This novel diagrammatic approach [1] follows from an earlier construction [4] of Witten which related perturbative amplitudes of conformal $\mathcal{N} = 4$ supersymmetric gauge theory in the large N_c limit to D-instanton contributions in a topological string theory in twistor space. The key observation of [1, 4] is that tree-level and also loop diagrams in SYM possess a tractable geometric structure when they are transformed from Minkowski to twistor space.

The results [1, 4] have been tested and further developed in gauge theory in [5–12], and in string theory and supergravity in [13–22].

The new perturbation theory involves scalar diagrams since MHV vertices are scalar quantities. They are linked together by scalar propagators at tree-level, and the internal lines are continued off-shell in a particular fashion. The final result for any particular amplitude can be shown to be Lorentz-covariant and is independent of the particular choice for the off-shell continuation. The authors of [1] derived new expressions for a class of tree amplitudes with three consecutive negative helicities and any number of positive ones. It already has been verified in [1] that the new scalar graph approach agrees with a number of known standard results for scattering amplitudes in pure gauge theory. Furthermore, it was shown in [5] that all $\overline{\text{MHV}}$ (or googly) amplitudes – i.e. amplitudes with two positive helicity gluons and an arbitrary number of negative ones – are reproduced correctly in the CSW formalism. Recursive relations for constructing generic tree-level non-MHV amplitudes in the CSW formalism were obtained in [8]. Moreover, general next-to-MHV gluonic amplitudes were derived in [9] at tree level. These are the amplitudes where any three of n gluons have negative helicities.

We conclude that there is sufficient evidence that the CSW method works correctly and remarkably well at tree level and for gluon-only amplitudes.

Given this and also the fact that at present there is no detailed derivation of the CSW rules either in gauge theory, or in string theory, we would like to see how the method works in more general settings. There is a number of questions one can ask about the CSW formalism from the gauge theory perspective:

(1) Does the CSW method work only in the pure gauge sector at tree level or can it be applied to supersymmetric theories?
(2) If the method does apply to supersymmetric theories, does it work in $\mathcal{N} = 1$ theory or in $\mathcal{N} = 4$ theory or in a generic supersymmetric Yang–Mills?
(3) Does it work for diagrams with fundamental quarks in a non-supersymmetric $SU(N)$ theory, i.e. in QCD?
(4) Can we work with a finite number of colors?
(5) Can the CSW approach be used for practical calculations of amplitudes needed in phenomenological applications?
(6) Ask the five questions listed above for amplitudes at loop level.

The goal of these notes is to discuss and answer some of these questions.

It is often said that any gauge theory at tree level behaves as if it was supersymmetric. More precisely, in a supersymmetric theory the non-supersymmetric sector and the superpartners are completely decoupled at tree level. This is because at tree level superpartners cannot propagate in loops. This observation, on its own, does not answer the question of how to relate amplitudes with quarks to amplitudes with gluinos. The color structures of these amplitudes are clearly different.[a]

In Section 2 we will briefly recall well-known results about the decomposition of full amplitudes into the color factor T_n and the purely kinematic partial amplitude A_n. A key point in the approach of [1, 4] is that only the kinematic amplitude A_n is evaluated directly. Since A_n does not contain color factors, it is the same for tree amplitudes involving quarks and for those with gluinos.

A priori, when comparing kinematic amplitudes in a non-supersymmetric and in a supersymmetric theory, we should make sure that both theories have a similar field content. In particular, when comparing kinematic amplitudes in QCD and in SYM, (at least initially) we need to restrict to the SYM theory with vectors, fermions and no scalars. Scalars are potentially dangerous, since they can propagate in the internal lines and spoil the agreement

[a] Also, amplitudes with gluons and gluinos are automatically planar at tree level. This is not the case for tree diagrams with quarks, as they contain $1/N$-suppressed terms in $SU(N)$ gauge theory.

between the amplitudes. Hence, while the kinematic tree-level amplitudes in massless QCD agree with those in $\mathcal{N}=1$ pure SYM, one might ask if the agreement is lost when comparing QCD amplitudes to amplitudes in $\mathcal{N}=4$ (and $\mathcal{N}=2$) theories. Fortunately, this is not the case, the agreement between multi-particle quark-gluon amplitudes in QCD and the corresponding gluino-gluon amplitudes in SYM theories does not depend on $\mathcal{N}$. The main point here is that in $\mathcal{N}=2$ and $\mathcal{N}=4$ theories, the scalars ϕ couple to gluinos Λ^A and Λ^B from different $\mathcal{N}=1$ supermultiplets,

$$S_{\rm Yukawa} = \; g_{\rm YM}\,{\rm tr}\,\Lambda^-_A[\phi^{AB},\Lambda^-_B] \;+\; g_{\rm YM}\,{\rm tr}\,\Lambda^{A+}[\overline{\phi}_{AB},\Lambda^{B+}]\;, \qquad (1)$$

where $A,B=1,\dots\mathcal{N}$, and $\phi^{AB}=-\phi^{BA}$, hence $A\neq B$. Meanwhile quarks are identified with gluinos of the same fixed A, i.e. $q\leftrightarrow\Lambda^{A=1\,+}$, $\overline{q}\leftrightarrow\Lambda^-_{A=1}$. QCD-amplitudes with m quarks, m antiquarks and l gluons in external lines correspond to SYM-amplitudes with m gluinos Λ^{1+}, m anti-gluinos Λ^-_1, and l gluons. Since all external (anti)-gluinos are from the same $\mathcal{N}=1$ supermultiplet, they cannot produce scalars in the internal lines of tree diagrams. These diagrams are all the same for all $\mathcal{N}=0,\dots,4$. Of course, in $\mathcal{N}=4$ and $\mathcal{N}=2$ theories there are other classes of diagrams with gluinos from different $\mathcal{N}=1$ supermultiplets, and also with scalars in external lines. Applications of the scalar graph approach to these more general classes of tree amplitudes in $\mathcal{N}=2,4$ SYM will be discussed in Sections 5 and 6.

Following [6] we conclude that, if the CSW formalism gives correct results for partial amplitudes A_n in a supersymmetric theory, it will also work in a nonsupersymmetric case, and for a finite number of colors. Full amplitudes are then determined uniquely from the kinematic part A_n, and the known expressions for T_n, given in Eqs. (4), (6) below. This means [6] that for tree amplitudes questions (1) and (3) are essentially the same, and we have a positive answer to question (4).

In Section 3 we will concentrate on tree-level non-MHV (NMHV) amplitudes with gluons only. We will review the CSW formalism [1] for calculating these amplitudes and note a technical subtlety which occurs in the calculation. There are unphysical singularities which occur in certain diagrams. They must cancel between individual contributions to physical amplitudes. These cancellations were carried out successfully in all known cases [1,6,9], but it is more desirable to avoid them altogether [10]. Purely gluonic amplitudes can be related via supersymmetric Ward identities to amplitudes containing fermions. The latter are free of unphysical singularities for generic phase space points and no further helicity-spinor algebra is required to convert the results into an immediately usable form. The main result of Section

3 is equation (25) which expresses purely gluonic amplitudes in terms of amplitudes with fermions which are free from unphysical singularities.

Calculations of amplitudes involving fermions were carried out in [10] and will be reproduced in later sections (7 and 8). But first we need to set up the formalism for the CSW scalar graph method in the presence of fermions (and scalars). A natural way to do this is to consider gauge theories with extended supersymmetry.

In Section 4 we will write down $\mathcal{N} = 4$ supersymmetry algebra in helicity basis which can be used for deriving supersymmetric Ward identities for generic $1 \leq \mathcal{N} \leq 4$ gauge theories.

In Section 5 we will present the analytic $\mathcal{N} = 4$ supervertex of Nair [23] which incorporates all the component vertices needed for the scalar graph formalism in generic gauge theories with gauge fields, fermions and scalars. We will see that, interestingly, all of the allowed vertices are not MHV in theories with scalars [10]. For example, $A_n(g^-, \Lambda^{1+}, \Lambda^{2+}, \Lambda^{3+}, \Lambda^{4+})$ is an analytic, but non-MHV amplitude in $\mathcal{N} = 4$ theory. This implies that the scalar graph approach is not primarily based on MHV amplitudes.

In Section 6 we will apply the scalar graph formalism for calculating three simple examples of $\overline{\text{MHV}}$ (or, more precisely, anti-analytic) amplitudes which involve fermions and gluons. In all cases we will reproduce known results for these anti-analytic amplitudes, which implies that at tree level the scalar graph method appears to work correctly not only in $\mathcal{N} = 0, 1$ theories, but also in full $\mathcal{N} = 2$ and $\mathcal{N} = 4$ SYM. In particular, the $\mathcal{N} = 4$ result (55) verifies the fact that the building blocks of the scalar graph method are indeed the analytic vertices (31), which can have less than 2 negative helicities, i.e. are not MHV.

General tree-level expressions for n-point amplitudes with three negative helicities carried by fermions and gluons were derived in [10]. We will reproduce these calculations in Sections 7 and 8. In Section 9 we will show how to calculate tree amplitudes with vectors, fermions and scalars compactly using the scalar graph method with the supervertex of Section 5.

In Section 10 we will briefly review the known applications of the CSW scalar graph approach for loops and Section 11 presents our conclusions.

In the original topological string theory formulation [4], one obtains tree-level amplitudes with $d + 1$ negative-helicity gluons from contributions of D-instantons of degree d. These include contributions from connected multi-instantons of degree-d and from d disconnected single instantons (as well as from all intermediate mixed cases of total degree d). The CSW formalism [1] is based on integrating only over the moduli space of completely disconnected

instantons of degree one, linked by twistor space propagators. Degree-one D-instantons in string theory correspond to MHV vertices, and obtaining amplitudes with an arbitrary number of negative helicities using MHV vertices is dual in twistor space to integrating over degree-one instantons.

In Refs. [13, 14] Roiban, Spradlin, and Volovich computed the integrals in the opposite regime – over the moduli space of connected D-instantons of degree d. They found that for $\overline{\text{MHV}}$ amplitudes, and certain next-to-MHV amplitudes these integrals correctly reproduce known expressions for gauge theory amplitudes. We therefore seem to have different ways of computing the amplitudes from the topological B model. These different prescriptions were reconciled on the string theory side in [18] by showing that the corresponding integrals over instanton moduli spaces can be reduced to an integral over the common boundary and are hence equivalent. On the field theory side, the equivalence of different prescriptions was explained in [8] as the freedom to choose different decompositions of any given NMHV tree diagram into smaller blocks of MHV and NMHV diagrams. In this paper we use the CSW formalism for computing gauge theory amplitudes. On the string theory side this corresponds to choosing the disconnected instantons prescription.

2. Tree Amplitudes

We will consider tree-level amplitudes in a generic $SU(N)$ gauge theory with an arbitrary finite number of colors. $SU(N)$ is unbroken and all fields are taken to be massless, we refer to them generically as gluons, fermions and scalars.

2.1. *Color decomposition*

It is well-known that a full n-point amplitude M_n can be represented as a sum of products of color factors T_n and purely kinematic partial amplitudes A_n,

$$M_n(\{k_i, h_i, c_i\}) \,=\, \sum_{\sigma} T_n(\{c_{\sigma(i)}\})\, A_n(\{k_{\sigma(i)}, h_{\sigma(i)}\})\,. \qquad (2)$$

Here $\{c_i\}$ are color labels of external legs $i = 1 \ldots n$, and the kinematic variables $\{k_i, h_i\}$ are on-shell external momenta and helicities: all $k_i^2 = 0$, and $h_i = \pm 1$ for gluons, $h_i = \pm\frac{1}{2}$ for fermions, and $h_i = 0$ for scalars. The sum in (2) is over appropriate simultaneous permutations σ of color labels $\{c_{\sigma(i)}\}$ and kinematic variables $\{k_{\sigma(i)}, h_{\sigma(i)}\}$. The color factors T_n are easy to determine, and the non-trivial information about the full amplitude

M_n is contained in the purely kinematic part A_n. If the partial amplitudes $A_n(\{k_i, h_i\})$ are known for all permutations σ of the kinematic variables, the full amplitude M_n can be determined from (2).

We first consider tree amplitudes with fields in the adjoint representation only (e.g. gluons, gluinos and no quarks). The color variables $\{c_i\}$ correspond to the adjoint representation indices, $\{c_i\} = \{a_i\}$, and the color factor T_n is a single trace of generators,

$$M_n^{\rm tree}(\{k_i, h_i, a_i\}) = \sum_\sigma {\rm tr}\left({\rm T}^{a_{\sigma(1)}} ... {\rm T}^{a_{\sigma(n)}}\right)\, A_n^{\rm tree}(k_{\sigma(1)}, h_{\sigma(1)}, ..., k_{\sigma(n)}, h_{\sigma(n)})\,. \tag{3}$$

Here the sum is over $(n-1)!$ noncyclic inequivalent permutations of n external particles. The single-trace structure in (3),

$$T_n \,=\, {\rm tr}\left({\rm T}^{a_1} \dots {\rm T}^{a_n}\right), \tag{4}$$

implies that all tree level amplitudes of particles transforming in the adjoint representation of $SU(N)$ are planar. This is not the case either for loop amplitudes, or for tree amplitudes involving fundamental quarks.

Fields in the fundamental representation couple to the trace $U(1)$ factor of the $U(N)$ gauge group. In passing to the $SU(N)$ case this introduces power-suppressed $1/N^p$ terms. However, there is a remarkable simplification for tree diagrams involving fundamental quarks; the factorization property (2) still holds. More precisely, for a fixed color ordering σ, the amplitude with m quark-antiquark pairs and l gluons is still a perfect product,

$$T_{l+2m}(\{c_{\sigma(i)}\})\; A_{l+2m}(\{k_{\sigma(i)}, h_{\sigma(i)}\})\,, \tag{5}$$

and all $1/N^p$ corrections to the amplitude are contained in the first term. For tree amplitudes the exact color factor in (5) is [24]

$$T_{l+2m} = \frac{(-1)^p}{N^p}\,({\rm T}^{a_1} \dots {\rm T}^{a_{l_1}})_{i_1\alpha_1}({\rm T}^{a_{l_1+1}} ... {\rm T}^{a_{l_2}})_{i_2\alpha_2} ... ({\rm T}^{a_{l_{m-1}+1}} ... {\rm T}^{a_l})_{i_m\alpha_m}\,. \tag{6}$$

Here $l_1, \dots, l_m$ correspond to an arbitrary partition of an arbitrary permutation of the l gluon indices; $i_1, \dots i_m$ are the color indices of quarks, and $\alpha_1, \dots \alpha_m$ of the antiquarks. In perturbation theory each external quark is connected by a fermion line to an external antiquark (all particles are counted as incoming). When quark i_k is connected by a fermion line to antiquark α_k, we set $\alpha_k = \bar{i_k}$. Thus, the set of $\alpha_1, \dots \alpha_m$ is a permutation of the set $\bar{i_1}, \dots \bar{i_m}$. Finally, the power p is equal to the number of times $\alpha_k = \bar{i_k}$ minus 1. When there is only one quark-antiquark pair, $m = 1$ and $p = 0$. For a general m, the power p in (6) varies from 0 to $m-1$.

The kinematic amplitudes A_{l+2m} in (5) have the color information stripped off and hence do not distinguish between fundamental quarks and adjoint gluinos. Thus,

$$A_{l+2m}(q,\ldots,\bar{q},\ldots,g^+,\ldots,g^-) \;=\; A_{l+2m}(\Lambda^+,\ldots,\Lambda^-,\ldots,g^+,\ldots,g^-)\,, \tag{7}$$

where q, $\bar{q}$, $g^{\pm}$, $\Lambda^{\pm}$ denote quarks, antiquarks, gluons and gluinos of $\pm$ helicity.

In the following sections we will use the scalar graph formalism of [1] to evaluate the kinematic amplitudes A_n in (7). Full amplitudes can then be determined uniquely from the kinematic part A_n, and the known expressions for T_n in (4) and (6) by summing over the inequivalent color orderings in (2).

From now on we concentrate on the purely kinematic part of the amplitude, A_n.

2.2. *Amplitudes in the spinor helicity formalism*

We will first consider theories with $\mathcal{N} \leq 1$ supersymmetry. Gauge theories with extended supersymmetry have a more intricate behavior of their amplitudes in the helicity basis and their study will be postponed until Section 4. Theories with $\mathcal{N} = 4$ (or $\mathcal{N} = 2$) supersymmetry have $\mathcal{N}$ different species of gluinos and 6 (or 4) scalar fields. This leads to a large number of elementary MHV-like vertices in the scalar graph formalism. This proliferation of elementary vertices asks for a super-graph generalization of the CSW scalar graph method, which will be outlined in Section 5 following Ref. [10].

Here we will concentrate on tree level partial amplitudes $A_n = A_{l+2m}$ with l gluons and $2m$ fermions in the helicity basis, and all external lines are defined to be incoming.

In $\mathcal{N} \leq 1$ theory a fermion of helicity $+\frac{1}{2}$ is always connected by a fermion propagator to a helicity $-\frac{1}{2}$ fermion hence the number of fermions $2m$ is always even. This statement is correct only in theories without scalar fields. In the $\mathcal{N} = 4$ theory, a pair of positive helicity fermions, Λ^{1+}, Λ^{2+}, can be connected to another pair of positive helicity fermions, Λ^{3+}, Λ^{4+}, by a scalar propagator.

In $\mathcal{N} \leq 1$ theory a tree amplitude A_n with less than two opposite helicities vanishes [b] identically [25]. The first nonvanishing amplitudes contain $n-2$ particles with helicities of the same sign [2,3] and are called maximal helicity violating (MHV) amplitudes.

[b] In the $\mathcal{N} = 1$ theory this is also correct to all orders in the loop expansion and non-perturbatively.

In the spinor helicity formalism [2, 3, 26] an on-shell momentum of a massless particle, $p_\mu p^\mu = 0$, is represented as

$$p_{a\dot{a}} \equiv \; p_\mu \sigma^\mu_{a\dot{a}} = \; \lambda_a \tilde{\lambda}_{\dot{a}} \; , \tag{8}$$

where λ_a and $\tilde{\lambda}_{\dot{a}}$ are two commuting spinors of positive and negative chirality. Spinor inner products are defined by [c]

$$\langle \lambda, \lambda' \rangle = \; \epsilon_{ab} \lambda^a \lambda'^b \; , \qquad [\tilde{\lambda}, \tilde{\lambda}'] = \; \epsilon_{\dot{a}\dot{b}} \tilde{\lambda}^{\dot{a}} \tilde{\lambda}'^{\dot{b}} \; , \tag{9}$$

and a scalar product of two null vectors, $p_{a\dot{a}} = \lambda_a \tilde{\lambda}_{\dot{a}}$ and $q_{a\dot{a}} = \lambda'_a \tilde{\lambda}'_{\dot{a}}$, becomes

$$p_\mu q^\mu = \; \frac{1}{2} \langle \lambda, \lambda' \rangle [\tilde{\lambda}, \tilde{\lambda}'] \; . \tag{10}$$

An MHV amplitude $A_n = A_{l+2m}$ with l gluons and $2m$ fermions in $\mathcal{N} \leq 1$ theories exists only for $m = 0, 1, 2$. This is because it must have precisely $n-2$ particles with positive and 2 with negative helicities, and our fermions always come in pairs with helicities $\pm\frac{1}{2}$. Hence, there are three types of MHV tree amplitudes in $\mathcal{N} \leq 1$ theories:

$$A_n(g_r^-, g_s^-) \; , \quad A_n(g_t^-, \Lambda_r^-, \Lambda_s^+) \; , \quad A_n(\Lambda_t^-, \Lambda_s^+, \Lambda_r^-, \Lambda_q^+) \; . \tag{11}$$

Suppressing the overall momentum conservation factor,

$$i g_{\rm YM}^{n-2} \, (2\pi)^4 \, \delta^{(4)}(\sum_{i=1}^n \lambda_{ia} \tilde{\lambda}_{i\dot{a}}) \; , \tag{12}$$

the MHV purely gluonic amplitude is [2,3]

$$A_n(g_r^-, g_s^-) = \; \frac{\langle \lambda_r, \lambda_s \rangle^4}{\prod_{i=1}^n \langle \lambda_i, \lambda_{i+1} \rangle} \equiv \; \frac{\langle r \; s \rangle^4}{\prod_{i=1}^n \langle i \; i+1 \rangle} \; , \tag{13}$$

where $\lambda_{n+1} \equiv \lambda_1$. The MHV amplitude with two external fermions and $n-2$ gluons is

$$\begin{aligned} A_n(g_t^-, \Lambda_r^-, \Lambda_s^+) &= \; \frac{\langle t \; r \rangle^3 \; \langle t \; s \rangle}{\prod_{i=1}^n \langle i \; i+1 \rangle} \; , \\ A_n(g_t^-, \Lambda_s^+, \Lambda_r^-) &= \; - \frac{\langle t \; r \rangle^3 \; \langle t \; s \rangle}{\prod_{i=1}^n \langle i \; i+1 \rangle} \; , \end{aligned} \tag{14}$$

where the first expression corresponds to $r < s$ and the second to $s < r$ (and t is arbitrary). The MHV amplitudes with four fermions and $n-4$ gluons

[c] Our conventions for spinor helicities follow [1, 4] and are the same as in [6, 10].

on external lines are

$$\begin{aligned} A_n(\Lambda_t^-, \Lambda_s^+, \Lambda_r^-, \Lambda_q^+) &= \frac{\langle t\ r\rangle^3\ \langle s\ q\rangle}{\prod_{i=1}^n \langle i\ i+1\rangle}\ , \\ A_n(\Lambda_t^-, \Lambda_r^-, \Lambda_s^+, \Lambda_q^+) &= -\frac{\langle t\ r\rangle^3\ \langle s\ q\rangle}{\prod_{i=1}^n \langle i\ i+1\rangle}\ . \end{aligned} \tag{15}$$

The first expression in (15) corresponds to $t < s < r < q$, the second to $t < r < s < q$, and there are other similar expressions, obtained by further permutations of fermions, with the overall sign determined by the ordering.

Expressions (14), (15) can be derived from supersymmetric Ward identities [24, 25, 27], and we will have more to say about this in Section 5. The $\overline{\text{MHV}}$ amplitude can be obtained, as always, by exchanging helicities $+ \leftrightarrow -$ and $\langle i\ j\rangle \leftrightarrow [i\ j]$.

3. Gluonic NMHV amplitudes and the CSW method

The formalism of CSW was developed in [1] for calculating purely gluonic amplitudes at tree level. In this approach all non-MHV n-gluon amplitudes (including $\overline{\text{MHV}}$) are expressed as sums of tree diagrams in an effective scalar perturbation theory. The vertices in this theory are the MHV amplitudes (13), continued off-shell as described below, and connected by scalar propagators $1/q^2$. It was shown in [6, 10] that the same idea continues to work in theories with fermions and gluons. Scattering amplitudes are determined from scalar diagrams with three types of MHV vertices, (13),(14) and (15), which are connected to each other with scalar propagators $1/q^2$. Also, since we have argued above that at tree level, supersymmetry is irrelevant, the method applies to supersymmetric and non-supersymmetric theories [6].

When one leg of an MHV vertex is connected by a propagator to a leg of another MHV vertex, both legs become internal to the diagram and have to be continued off-shell. Off-shell continuation is defined as follows [1]: we pick an arbitrary spinor $\xi^{\dot a}_{\rm Ref}$ and define λ_a for any internal line carrying momentum $q_{a\dot a}$ by

$$\lambda_a = q_{a\dot a}\xi^{\dot a}_{\rm Ref}\ . \tag{16}$$

External lines in a diagram remain on-shell, and for them λ is defined in the usual way. For the off-shell lines, the same $\xi_{\rm Ref}$ is used in all diagrams contributing to a given amplitude.

For practical applications the authors of [1] have chosen $\xi^{\dot a}_{\rm Ref}$ in (16) to be equal to $\tilde\lambda^{\dot a}$ of one of the external legs of negative helicity, e.g. the first one,

$$\xi^{\dot a}_{\rm Ref} = \tilde\lambda^{\dot a}_1\ . \tag{17}$$

This corresponds to identifying the reference spinor with one of the kinematic variables of the theory. The explicit dependence on the reference spinor $\xi^{\dot{a}}_{\rm Ref}$ disappears and the resulting expressions for all scalar diagrams in the CSW approach are functions only of the kinematic variables $\lambda_{i\,a}$ and $\tilde{\lambda}^{\dot{a}}_i$. This means that the expressions for all individual diagrams automatically appear to be Lorentz-invariant (in the sense that they do not depend on an external spinor $\xi^{\dot{a}}_{\rm Ref}$) and also gauge-invariant (since the reference spinor corresponds to the axial gauge fixing $\xi^{\mu}_{\rm Ref}A_\mu = 0$, where $\xi^{\dot{a}a}_{\rm Ref} = \xi^{\dot{a}}_{\rm Ref}\xi^{a}_{\rm Ref}$).

There is a price to pay for this invariance of the individual diagrams. Equations (16), (17) lead to unphysical singularities [d] which occur for the whole of phase space and which have to be cancelled between the individual diagrams. The result for the total amplitude is, of course, free of these unphysical singularities, but their cancellation and the retention of the finite part requires some work, see [1] and section 3.1 of [6].

Following [6, 10] we note that these unphysical singularities are specific to the three-gluon MHV vertices and, importantly, they do not occur in any of the MHV vertices involving a fermion field. To see how these singularities arise in gluon vertices, consider a 3-point MHV vertex,

$$A_3(g_1^-, g_2^-, g_3^+) = \frac{\langle 1\ 2\rangle^4}{\langle 1\ 2\rangle\langle 2\ 3\rangle\langle 3\ 1\rangle} = \frac{\langle 1\ 2\rangle^3}{\langle 2\ 3\rangle\langle 3\ 1\rangle}\ . \tag{18}$$

This vertex exists only when one of the legs is off-shell. Take it to be the g_3^+ leg. Then Eqs. (16), (17), and momentum conservation, $q = p_1 + p_2$, give

$$\lambda_{3\,a} = (p_1 + p_2)_{a\dot{a}}\,\tilde{\lambda}^{\dot{a}}_1 = -\lambda_{1\,a}\,[1\ 1] - \lambda_{2\,a}\,[2\ 1] = -\lambda_{2\,a}\,[2\ 1]\ . \tag{19}$$

This implies that $\langle 2\ 3\rangle = -\langle 2\ 2\rangle[2\ 1] = 0$, and the denominator of (18) vanishes. This is precisely the singularity we are after. If instead of the g_3^+ leg, one takes the g_2^- leg go off-shell, then, $\langle 2\ 3\rangle = -\langle 3\ 3\rangle[3\ 1] = 0$ again.

Now consider a three-point MHV vertex involving two fermions and a gluon,

$$A_3(\Lambda_1^-, g_2^-, \Lambda_3^+) = \frac{\langle 2\ 1\rangle^3\langle 2\ 3\rangle}{\langle 1\ 2\rangle\langle 2\ 3\rangle\langle 3\ 1\rangle} = -\frac{\langle 2\ 1\rangle^2}{\langle 3\ 1\rangle}\ . \tag{20}$$

Choose the reference spinor to be as before, $\tilde{\lambda}^{\dot{a}}_1$, and take the second or the third leg off-shell. This again makes $\langle 2\ 3\rangle = 0$, but now the factor of $\langle 2\ 3\rangle$ is cancelled on the right hand side of (20). Hence, the vertex (20) is regular, and there are no unphysical singularities in the amplitudes involving at least one

[d] Unphysical means that these singularities are not the standard IR soft and collinear divergences in the amplitudes.

negative helicity fermion when it's helicity is chosen to be the reference spinor [6]. One concludes that the difficulties with singularities at intermediate stages of the calculation occur only in purely gluonic amplitudes. One way to avoid these intermediate singularities is to choose an off-shell continuation different from the CSW prescription (16),(17).

Recently, Kosower [9] used an off-shell continuation by projection of the off-shell momentum with respect to an on-shell reference momentum $q^{\mu}_{\rm Ref}$, to derive, for the first time, an expression for a general NMHV amplitude with three negative helicity gluons. The amplitude in [9] was from the start free of unphysical divergences, however it required a certain amount of spinor algebra to bring it into a form independent of the reference momentum.

In [10] we proposed another simple method for finding all purely gluonic NMHV amplitudes. Using $\mathcal{N}=1$ supersymmetric Ward identities one can relate purely gluonic amplitudes to a linear combination of amplitudes with one fermion–antifermion pair. As explained above, the latter are free of singularities and are manifestly Lorentz-invariant. These fermionic amplitudes will be calculated in Section 7 using the CSW scalar graph approach with fermions [6] and following [10].

To derive supersymmetric Ward identities [25] we use the fact that supercharges Q annihilate the vacuum and consider the equation,

$$\langle [Q\,,\,\Lambda_k^+ \ldots g_{r_1}^- \ldots g_{r_2}^- \ldots g_{r_3}^- \ldots] \rangle \;=\; 0\;, \tag{21}$$

where dots indicate positive helicity gluons. In order to make the anticommuting spinor Q a singlet entering a commutative (rather than anticommutative) algebra with all the fields, we contract it with a commuting spinor η and multiply it by a Grassmann number θ. This defines a commuting singlet operator $Q(\eta)$. Following [27] we can write down the following susy algebra relations,

$$\begin{aligned} [Q(\eta)\,,\,\Lambda^+(k)] \;&=\; -\theta\langle \eta\; k\rangle\, g^+(k)\;, \quad [Q(\eta)\,,\,\Lambda^-(k)] \;=\; +\theta[\eta\; k]\, g^-(k)\;, \\ [Q(\eta)\,,\,g^-(k)] \;&=\; +\theta\langle \eta\; k\rangle\, \Lambda^-(k)\;, \quad [Q(\eta)\,,\,g^+(k)] \;=\; -\theta[\eta\; k]\, \Lambda^+(k)\;. \end{aligned} \tag{22}$$

In what follows, the anticommuting parameter θ will cancel from the relevant expressions for the amplitudes. The arbitrary spinors η_a, $\eta_{\dot a}$, will be fixed below. It then follows from (22) that

$$\begin{aligned} \langle \eta\; k\rangle\, A_n(g_{r_1}^-, g_{r_2}^-, g_{r_3}^-) = \;& \langle \eta\; r_1\rangle\, A_n(\Lambda_k^+, \Lambda_{r_1}^-, g_{r_2}^-, g_{r_3}^-) \\ &+ \langle \eta\; r_2\rangle\, A_n(\Lambda_k^+, g_{r_1}^-, \Lambda_{r_2}^-, g_{r_3}^-) + \langle \eta\; r_3\rangle\, A_n(\Lambda_k^+, g_{r_1}^-, g_{r_2}^-, \Lambda_{r_3}^-)\;. \end{aligned} \tag{23}$$

After choosing η to be one of the three r_j we find from (23) that the purely gluonic amplitude with three negative helicities is given by a sum of two

fermion-antifermion-gluon-gluon amplitudes. Note that in the expressions above and in what follows, in n-point amplitudes we show only the relevant particles, and suppress all the positive helicity gluons g^+.

Remarkably, this approach works for any number of negative helicities, and the NMHV amplitude with h negative gluons is expressed via a simple linear combination of $h-1$ NMHV amplitudes with one fermion-antifermion pair.

In Sections 7 and 8 we will evaluate NMHV amplitudes with fermions. In particular, in Section 7 we will calculate the following three amplitudes,

$$A_n(\Lambda^-_{m_1}, g^-_{m_2}, g^-_{m_3}, \Lambda^+_k)\,, \quad A_n(\Lambda^-_{m_1}, g^-_{m_2}, \Lambda^+_k, g^-_{m_3})\,, \quad A_n(\Lambda^-_{m_1}, \Lambda^+_k, g^-_{m_2}, g^-_{m_3})\,. \tag{24}$$

In terms of these, the purely gluonic amplitude of (23) reads

$$\begin{aligned} A_n(g^-_{r_1}, g^-_{r_2}, g^-_{r_3}) = &-\frac{\langle \eta\ r_1\rangle}{\langle \eta\ k\rangle}\ A_n(\Lambda^-_{m_1}, g^-_{m_2}, g^-_{m_3}, \Lambda^+_k)|_{m_1=r_1, m_2=r_2, m_3=r_3} \\ &-\frac{\langle \eta\ r_2\rangle}{\langle \eta\ k\rangle}\ A_n(\Lambda^-_{m_1}, g^-_{m_2}, \Lambda^+_k, g^-_{m_3})|_{m_1=r_2, m_2=r_3, m_3=r_1} \\ &-\frac{\langle \eta\ r_3\rangle}{\langle \eta\ k\rangle}\ A_n(\Lambda^-_{m_1}, \Lambda^+_k, g^-_{m_2}, g^-_{m_3})|_{m_1=r_3, m_2=r_1, m_3=r_2}\ , \end{aligned} \tag{25}$$

and η can be chosen to be one of the three m_j to further simplify this formula.

4. $\mathcal{N}=4$ Supersymmetry Algebra in Helicity Formalism

The $\mathcal{N}=1$ susy algebra relations (22) can be generalized to $\mathcal{N}\geq 1$ theories. The $\mathcal{N}=4$ susy relations read:

$$[Q^A(\eta)\,,\, g^+(k)] \;=\; -\theta_A[\eta\ k]\,\Lambda^{+\,A}(k)\,, \tag{26a}$$

$$[Q^A(\eta)\,,\, \Lambda^{+\,B}(k)] \;=\; -\delta^{AB}\,\theta_A\langle\eta\ k\rangle\, g^+(k) \,-\, \theta_A[\eta\ k]\,\phi^{AB}\,, \tag{26b}$$

$$[Q^A(\eta)\,,\, \overline{\phi}_{AB}(k)] \;=\; -\theta_A[\eta\ k]\,\Lambda^-_B(k)\,, \tag{26c}$$

$$[Q_A(\eta)\,,\, \phi^{AB}(k)] \;=\; \theta_A\langle\eta\ k\rangle\,\Lambda^{+\,B}(k)\,, \tag{26d}$$

$$[Q_A(\eta)\,,\, \Lambda^-_B(k)] \;=\; \delta_{AB}\,\theta_A[\eta\ k]\, g^-(k) \,+\, \theta_A\langle\eta\ k\rangle\,\overline{\phi}_{AB}(k)\,, \tag{26e}$$

$$[Q_A(\eta)\,,\, g^-(k)] \;=\; \theta_A\langle\eta\ k\rangle\,\Lambda^-_A(k)\,. \tag{26f}$$

Our conventions are the same as in (22), and it is understood that $Q_A = Q^A$ and there is no summation over A in (26c), (26d). The conjugate scalar field is defined in the standard way,

$$\overline{\phi}_{AB} \;=\; \tfrac{1}{2}\,\epsilon_{ABCD}\,\phi^{CD} \;=\; (\phi^{AB})^\dagger\,. \tag{27}$$

Relations (26a)-(26f) can be used in order to derive $\mathcal{N}=2$ and $\mathcal{N}=4$ susy Ward identities which relate different classes of amplitudes in gauge theories with extended supersymmetry.

5. The Analytic Supervertex in $\mathcal{N}=4$ SYM

So far we have encountered three types of MHV amplitudes (13), (14) and (15). The key feature which distinguishes these amplitudes is the fact that they depend only on $\langle\lambda_i\ \lambda_j\rangle$ spinor products, and not on $[\tilde{\lambda}_i\ \tilde{\lambda}_i]$. We will call such amplitudes analytic.

All analytic amplitudes in generic $0 \leq \mathcal{N} \leq 4$ gauge theories can be combined into a single $\mathcal{N}=4$ supersymmetric expression of Nair [23],

$$A_n^{\mathcal{N}=4} = \ \delta^{(8)}\Big(\sum_{i=1}^{n}\lambda_{ia}\eta_i^A\Big)\ \frac{1}{\prod_{i=1}^{n}\langle i\ i+1\rangle}\ . \tag{28}$$

Here η_i^A are anticommuting variables and $A=1,2,3,4$. The Grassmann-valued delta function is defined in the usual way,

$$\delta^{(8)}\Big(\sum_{i=1}^{n}\lambda_{ia}\eta_i^A\Big) \equiv \ \prod_{A=1}^{4}\ \tfrac{1}{2}\Big(\sum_{i=1}^{n}\lambda_i^a\eta_i^A\Big)\Big(\sum_{i=1}^{n}\lambda_{ia}\eta_i^A\Big)\ . \tag{29}$$

Taylor expanding (28) in powers of η_i, one can identify each term in the expansion with a particular tree-level analytic amplitude in the $\mathcal{N}=4$ theory. $(\eta_i)^k$ for $k=0,\ldots,4$ is interpreted as the i^{th} particle with helicity $h_i = 1-\frac{k}{2}$. This implies that helicities take values, $\{1, \frac{1}{2}, 0, -\frac{1}{2}, -1\}$, which precisely correspond to those of the $\mathcal{N}=4$ supermultiplet, $\{g^-, \lambda_A^-, \phi^{AB}, \Lambda^{A+}, g^+\}$.

It is straightforward to write down a general rule [6] for associating a power of η with all component fields in $\mathcal{N}=4$,

$$g_i^- \sim \eta_i^1\eta_i^2\eta_i^3\eta_i^4\ ,\ \Lambda_1^- \sim -\eta_i^2\eta_i^3\eta_i^4\ ,\ \phi_i^{AB} \sim \eta_i^A\eta_i^B\ ,\ \Lambda_i^{A+} \sim \eta_i^A\ ,\ g_i^+ \sim 1\ , \tag{30}$$

with expressions for the remaining Λ_A^- with $A=2,3,4$ written in the same manner as the expression for Λ_1^- in (30). The first MHV amplitude (13) is derived from (28) by using the dictionary (30) and by selecting the $(\eta_r)^4\,(\eta_s)^4$ term in (28). The second amplitude (14) follows from the $(\eta_t)^4(\eta_r)^3(\eta_s)^1$ term in (28); and the third amplitude (15) is an $(\eta_r)^3(\eta_s)^1(\eta_t)^3(\eta_q)^1$ term.

There is a large number of such component amplitudes for an extended susy Yang–Mills, and what is remarkable, not all of these amplitudes are MHV. The analytic amplitudes of the $\mathcal{N}=4$ SYM obtained from (28), (30)

are [10]:

$$
\begin{aligned}
&A_n(g^-,g^-)\ , \quad A_n(g^-,\Lambda_A^-,\Lambda^{A+})\ , \quad A_n(\Lambda_A^-,\Lambda_B^-,\Lambda^{A+},\Lambda^{B+})\ ,\\
&A_n(g^-,\Lambda^{1+},\Lambda^{2+},\Lambda^{3+},\Lambda^{4+})\ , \quad A_n(\Lambda_A^-,\Lambda^{A+},\Lambda^{1+},\Lambda^{2+},\Lambda^{3+},\Lambda^{4+})\ ,\\
&A_n(\Lambda^{1+},\Lambda^{2+},\Lambda^{3+},\Lambda^{4+},\Lambda^{1+},\Lambda^{2+},\Lambda^{3+},\Lambda^{4+})\ ,\\
&A_n(\overline{\phi}_{AB},\Lambda^{A+},\Lambda^{B+},\Lambda^{1+},\Lambda^{2+},\Lambda^{3+},\Lambda^{4+})\ ,\\
&A_n(g^-,\overline{\phi}_{AB},\phi^{AB})\ , \quad A_n(g^-,\overline{\phi}_{AB},\Lambda^{A+},\Lambda^{B+})\ , \quad A_n(\Lambda_A^-,\Lambda_B^-,\phi^{AB})\ ,\\
&A_n(\Lambda_A^-,\phi^{AB},\overline{\phi}_{BC},\Lambda^{C+})\ , \quad A_n(\Lambda_A^-,\overline{\phi}_{BC},\Lambda^{A+},\Lambda^{B+},\Lambda^{C+})\ ,\\
&A_n(\overline{\phi},\phi,\overline{\phi},\phi)\ , \quad A_n(\overline{\phi},\phi,\overline{\phi},\Lambda^+,\Lambda^+)\ , \quad A_n(\overline{\phi},\overline{\phi},\Lambda^+,\Lambda^+,\Lambda^+,\Lambda^+)\ ,
\end{aligned}
\tag{31}
$$

where it is understood that $\overline{\phi}_{AB} = \frac{1}{2}\epsilon_{ABCD}\phi^{CD}$. In Eqs. (31) we do not distinguish between the different particle orderings in the amplitudes. The labels refer to supersymmetry multiplets, $A, B = 1, \ldots, 4$. Analytic amplitudes in (31) include the familiar MHV amplitudes, (13), (14), (15), as well as more complicated classes of amplitudes with external gluinos Λ^A, $\Lambda^{B\neq A}$, etc, and with external scalar fields ϕ^{AB}.

The second, third and fourth lines in (31) are not even MHV amplitudes; they have less than two negative helicities, and nevertheless, these amplitudes are non-vanishing in $\mathcal{N} = 4$ SYM. The conclusion we draw [10] is that in the scalar graph formalism in $\mathcal{N} \leq 4$ SYM, the amplitudes are characterized not by a number of negative helicities, but rather by the total number of η's associated to each amplitude via the rules (30).

All the analytic amplitudes listed in (31) can be calculated directly from (28), (30). There is a simple algorithm for doing this [10].

(1) For each amplitude in (31) substitute the fields by their η-expressions (30). There are precisely eight η's for each analytic amplitude.
(2) Keeping track of the overall sign, rearrange the anticommuting η's into a product of four pairs, $(\text{sign}) \times \eta_i^1\eta_j^1\,\eta_k^2\eta_l^2\,\eta_m^3\eta_n^3\,\eta_r^4\eta_s^4$.
(3) The amplitude is obtained by replacing each pair $\eta_i^A\eta_j^A$ by the spinor product $\langle i\ j\rangle$ and dividing by the usual denominator,

$$
A_n = \ (\text{sign}) \times \frac{\langle i\ j\rangle\langle k\ l\rangle\langle m\ n\rangle\langle r\ s\rangle}{\prod_{l=1}^{n}\ \langle l\ l+1\rangle}\ . \tag{32}
$$

In this way one can immediately write down expressions for all component amplitudes in (31). It can be checked that these expressions are inter-related via $\mathcal{N} = 4$ susy Ward identities which follow from the $\mathcal{N} = 4$ susy algebra in (26a)-(26f).

The vertices of the scalar graph method are the analytic vertices (31) which are all of degree-8 in η and are not necessarily MHV. These are component vertices of a single analytic supervertex [e] (28). The analytic amplitudes of degree-8 are the elementary blocks of the scalar graph approach. The next-to-minimal case are the amplitudes of degree-12 in η, and they are obtained by connecting two analytic vertices of [23] with a scalar propagator $1/q^2$. Each analytic vertex contributes 8 η's and a propagator removes 4. Scalar diagrams with three degree-8 vertices give the degree-12 amplitude, etc. In general, all n-point amplitudes are characterized by a degree $8, 12, 16, \ldots, (4n-8)$ which are obtained from scalar diagrams with $1, 2, 3, \ldots$ analytic vertices.[f] In Section 9 we will derive a simple expression for the first iteration of the degree-8 vertex. This iterative process can be continued straightforwardly to higher orders.

6. Calculating Simple Anti-Analytic Amplitudes

To show the simplicity of the scalar graph method at tree level and to test its results, in this section we will calculate some simple anti-analytic amplitudes of η-degree-12. More complicated general cases are discussed in Sections 7 – 9.

We work in $\mathcal{N}=1$, $\mathcal{N}=2$ and $\mathcal{N}=4$ SYM theories, and study

$$A_5^{\mathcal{N}=1}(g_1^-, \Lambda^-_{(1)\,2}, \Lambda^-_{(1)\,3}, \Lambda_4^{(1)+}, \Lambda_5^{(1)+}) \ , \tag{33a}$$

$$A_5^{\mathcal{N}=2}(\Lambda^-_{(1)\,1}, \Lambda^-_{(2)\,2}, g_3^-, \Lambda_4^{(1)+}, \Lambda_5^{(2)+}) \ , \tag{33b}$$

$$A_5^{\mathcal{N}=4}(\Lambda^-_{(1)\,1}, \Lambda^-_{(2)\,2}, \Lambda^-_{(3)\,3}, \Lambda^-_{(4)\,4}, g_5^+) \ , \tag{33c}$$

using the scalar graph method with analytic vertices. The labels $\mathcal{N}=1,2,4$ on the three amplitudes above correspond to the *minimal* number of supersymmetries for the given amplitude. In this section the $\mathcal{N}$-supersymmetry labels A, B are shown as (A) and (B).

In all cases we will reproduce known results for these anti-analytic amplitudes, which implies that at tree level the scalar graph method appears to work correctly not only in $\mathcal{N}=0,1$ theories, but also in full $\mathcal{N}=2$ and $\mathcal{N}=4$ SYM. This answers the question (2) in the introduction.

[e] The list of component vertices (31) is obtained by writing down all partitions of 8 into groups of 4, 3, 2 and 1. For example, $A_n(g^-, \overline{\phi}_{AB}, \Lambda^{A+}, \Lambda^{B+})$ follows from $8 = 4+2+1+1$.

[f] In practice, one needs to know only the first half of these amplitudes, since degree-$(4n-8)$ amplitudes are anti-analytic (also known as googly) and they are simply given by degree-8^* amplitudes, similarly degree-$(4n-12)$ are given by degree-12^*, etc.

Furthermore, the $\mathcal{N}=4$ result (55) for the amplitude (33c) will verify the fact that the building blocks of the scalar graph method are indeed the analytic vertices (31), which can have less than 2 negative helicities, i.e. are not MHV.

We will be using the of-shell prescription $\xi^{\dot{a}}_{\rm Ref} = \tilde{\lambda}^{\dot{a}}_2$ as in Section 3. Since in our amplitudes, the reference spinor $\tilde{\lambda}^{\dot{a}}_2$ always corresponds to a gluino $\Lambda-$, rather than a gluon g^-, there will be no singularities in our formulae at any stage of the calculation.

6.1. *Anti-analytic $\mathcal{N}=1$ amplitude*

There are three diagrams contributing to the first amplitude, Eq. (33a). The first one is a gluon exchange between two 2-fermion MHV-vertices. This diagram has a schematic form,

$$A_4(g_1^-,\Lambda_2^-,\underline{g_I^+},\Lambda_5^+)\ \frac{1}{q_I^2}\ A_3(\Lambda_3^-,\Lambda_4^+,\underline{g_{-I}^-})\ . \tag{34}$$

Here $\underline{g_I^+}$ and $\underline{g_{-I}^-}$ are off-shell (internal) gluons which are Wick-contracted via a scalar propagator, and $I=(3,4)$, which means, $\lambda_I=(p_3+p_4)\cdot\tilde{\lambda}_2$.

The second and the third diagrams involve a fermion exchange between a 2-fermion and a 4-fermion MHV vertices. They are given, respectively by

$$A(\Lambda_2^-,\Lambda_3^-,\Lambda_4^+,\underline{\Lambda_{-I}^+})\ \frac{1}{q_I^2}\ A(\Lambda_5^+,g_1^-,\underline{\Lambda_I^-})\ , \tag{35}$$

with $I=(2,4)$, and

$$A(g_1^-,\Lambda_2^-,\underline{\Lambda_I^+})\ \frac{1}{q_I^2}\ A(\Lambda_3^-,\Lambda_4^+,\Lambda_5^+,\underline{\Lambda_{-I}^-})\ , \tag{36}$$

with $I=(3,5)$. Both expressions, (35) and (36), are written in the form which is in agreement with the ordering prescription of [6] for internal fermions, $\mathrm{ket}^+\ \mathrm{ket}^-$. All three contributions are straightforward to evaluate using the relevant expressions for the component analytic vertices. These expressions follow from the algorithm (32).

1. The first contribution, Eq. (34), is

$$\begin{aligned}&\frac{-\langle 1\ 2\rangle^2}{(\langle 2\ 3\rangle[2\ 3]+\langle 2\ 4\rangle[2\ 4])\langle 5\ 1\rangle[2\ 1]}\cdot\frac{1}{\langle 3\ 4\rangle[3\ 4]}\cdot\langle 4\ 3\rangle[2\ 4]^2\\ &=\ \frac{[2\ 4]^2\langle 1\ 2\rangle^2}{[3\ 4](\langle 2\ 3\rangle[2\ 3]+\langle 2\ 4\rangle[2\ 4])\langle 5\ 1\rangle[2\ 1]}\ .\end{aligned} \tag{37}$$

2. The second diagram, Eq. (35), gives

$$\begin{aligned}&\frac{-\langle 2\ 3\rangle^2}{(\langle 2\ 3\rangle[2\ 3]+\langle 2\ 4\rangle[2\ 4])\langle 3\ 4\rangle}\cdot\frac{1}{\langle 5\ 1\rangle[5\ 1]}\cdot\frac{\langle 5\ 1\rangle[2\ 5]^2}{[2\ 1]}\\ &=\ \frac{-[2\ 5]^2\langle 2\ 3\rangle^2}{[2\ 1][5\ 1](\langle 2\ 3\rangle[2\ 3]+\langle 2\ 4\rangle[2\ 4])\langle 3\ 4\rangle}\ .\end{aligned}\tag{38}$$

3. The third contribution, Eq. (36), is

$$\frac{\langle 2\ 1\rangle}{[2\ 1]}\cdot\frac{1}{\langle 1\ 2\rangle[1\ 2]}\cdot\frac{\langle 3\ 1\rangle^2[2\ 1]}{\langle 3\ 4\rangle\langle 5\ 1\rangle}\ =\ \frac{\langle 3\ 1\rangle^2}{[2\ 1]\langle 3\ 4\rangle\langle 5\ 1\rangle}\ .\tag{39}$$

Now, we need to add up the three contributions. We first combine the expressions in (37) and (38) into

$$\frac{[4\ 5]^2}{[2\ 1][3\ 4][5\ 1]}-\frac{\langle 3\ 1\rangle^2}{[2\ 1]\langle 3\ 4\rangle\langle 5\ 1\rangle}\tag{40}$$

using momentum conservation identities, and the fact that $\langle 2\ 3\rangle[2\ 3]+\langle 2\ 4\rangle[2\ 4]\ =\ -\langle 3\ 4\rangle[3\ 4]+\langle 5\ 1\rangle[5\ 1]$. Then, adding the remaining contribution (39) we obtain the final result for the amplitude,

$$A_5^{\mathcal{N}=1}(g_1^-,\Lambda^-_{(1)\,2},\Lambda^-_{(1)\,3},\Lambda_4^{(1)+},\Lambda_5^{(1)+})\ =\ \frac{-[4\ 5]^3[2\ 3]}{[1\ 2][2\ 3][3\ 4][4\ 5][5\ 1]}\ .\tag{41}$$

which is precisely the right answer for the anti-analytic 5-point 'mostly minus' diagram. This can be easily verified by taking a complex conjugation (parity transform) of the corresponding analytic expression.

6.2. *Anti-analytic $\mathcal{N}=2$ amplitude*

There are three contributions to the amplitude (33b) The first contribution is a scalar exchange between two analytic vertices,

$$A_3(\Lambda^-_{(1)\,1},\Lambda^-_{(2)\,2},\underline{\phi^{(12)}_{-I}})\ \frac{1}{q_I^2}\ A_4(g_3^-,\Lambda_4^{(1)+},\Lambda_5^{(2)+},\underline{\phi_{(12)\,I}})\ .\tag{42}$$

Here $\underline{\phi^{(12)}_{-I}}$ and $\underline{\phi_{(12)\,I}}\equiv\underline{\phi^{(34)}_{I}}$ are off-shell (internal) scalars which are Wick-contracted. The external index $I=(1,2)$, which implies $\lambda_I=(p_1+p_2)\cdot\tilde\lambda_2=p_1\cdot\tilde\lambda_2$. The second contribution to (33b) is a fermion exchange,

$$A_3(g_3^-,\Lambda_4^{(1)+},\underline{\Lambda^-_{(1)\,-I}})\ \frac{1}{q_I^2}\ A_4(\Lambda_5^{(2)+},\Lambda^-_{(1)\,1},\Lambda^-_{(2)\,2},\underline{\Lambda_I^{(1)+}})\ ,\tag{43}$$

with external index $I=(3,4)$, that is, $\lambda_I=(p_3+p_4)\cdot\tilde\lambda_2$.

The final third contribution is again a fermion exchange,

$$A_3(\Lambda^-_{(2)\,2}, g_3^-, \underline{\Lambda^{(2)+}_{-I}})\ \frac{1}{q_I^2}\ A_4(\Lambda_4^{(1)+}, \Lambda_5^{(2)+}, \Lambda^-_{(1)\,1}, \underline{\Lambda^-_{(2)\,I}})\ , \tag{44}$$

with $I = (2,3)$, and $\lambda_I = (p_2 + p_3)\cdot\tilde{\lambda}_2 = p_3\cdot\tilde{\lambda}_2$. As before, all three contributions are straightforward to evaluate using the rules (32).

1. The first contribution, Eq. (42), is

$$\langle 1\ 2\rangle\ \cdot\ \frac{1}{\langle 1\ 2\rangle[1\ 2]}\ \cdot\ \frac{-\langle 3\ 5\rangle\langle 3\ 1\rangle[2\ 1]}{\langle 4\ 5\rangle\langle 5\ 1\rangle[2\ 1]}\ =\ \frac{\langle 3\ 5\rangle\langle 3\ 1\rangle}{\langle 4\ 5\rangle\langle 5\ 1\rangle}\frac{1}{[2\ 1]}\ . \tag{45}$$

2. The second contribution (43) gives

$$\frac{\langle 3\ 4\rangle^2[2\ 4]^2}{\langle 4\ 3\rangle[2\ 3]}\ \cdot\ \frac{1}{\langle 3\ 4\rangle[3\ 4]}\ \cdot\ \frac{-\langle 1\ 2\rangle}{\langle 5\ 1\rangle[2\ 1]}\ =\ -\ \frac{\langle 1\ 2\rangle}{\langle 5\ 1\rangle}\frac{[2\ 4]^2}{[1\ 2][2\ 3][3\ 4]}\ . \tag{46}$$

3. The third contribution (44), is

$$-\ \frac{\langle 2\ 3\rangle^2}{\langle 2\ 3\rangle[3\ 2]}\ \cdot\ \frac{1}{\langle 2\ 3\rangle[2\ 3]}\ \cdot\ \frac{\langle 1\ 3\rangle[2\ 3]}{\langle 4\ 5\rangle}\ =\ \frac{\langle 1\ 3\rangle}{\langle 4\ 5\rangle}\frac{1}{[2\ 3]}\ . \tag{47}$$

Now, we add up the three contributions in Eqs. (45), (46), (47) and using the momentum conservation identities obtain

$$A_5^{\mathcal{N}=2}(\Lambda^-_{(1)\,1}, \Lambda^-_{(2)\,2}, g_3^-, \Lambda_4^{(1)+}, \Lambda_5^{(2)+}) =\ \frac{[2\ 4][4\ 5]}{[1\ 2][2\ 3][3\ 4]}\ , \tag{48}$$

which is the correct result for the anti-analytic amplitude.

6.3. *Anti-analytic $\mathcal{N} = 4$ amplitude*

The amplitude $A_5^{\mathcal{N}=4}(\Lambda^-_{(1)\,1}, \Lambda^-_{(2)\,2}, \Lambda^-_{(3)\,3}, \Lambda^-_{(4)\,4}, g_5^+)$ receives contributions only from diagrams with a scalar exchange. There are three such diagrams.

The first one is

$$A_4(g_5^+, \Lambda^-_{(1)\,1}, \Lambda^-_{(2)\,2}, \underline{\phi^{(12)}_{-I}})\ \frac{1}{q_I^2}\ A_3(\Lambda^-_{(3)\,3}, \Lambda^-_{(4)\,4}, \underline{\phi^{(34)}_{I}})\ . \tag{49}$$

Here $\underline{\phi^{(12)}_{-I}}$ and $\underline{\phi^{(34)}_{I}}$ are off-shell (internal) scalars which are Wick-contracted and $\lambda_I = (p_1 + p_2 + p_5)\cdot\tilde{\lambda}_2 = (p_1 + p_5)\cdot\tilde{\lambda}_2$.

The second contribution to (33c) is

$$A_3(\Lambda^-_{(1)\,1}, \Lambda^-_{(2)\,2}, \underline{\phi^{(12)}_{-I}})\ \frac{1}{q_I^2}\ A_4(\Lambda^-_{(3)\,3}, \Lambda^-_{(4)\,4}, g_5^+, \underline{\phi^{(34)}_{I}})\ , \tag{50}$$

with external index $I = (1,2)$, that is, $\lambda_I = (p_1 + p_2)\cdot\tilde{\lambda}_2 = p_1\cdot\tilde{\lambda}_2$.

The third diagram gives,

$$A_3(\Lambda^-_{(2)\,2},\Lambda^-_{(3)\,3},\underline{\phi^{(23)}_{-I}})\ \frac{1}{q_I^2}\ A_4(\Lambda^-_{(4)\,4},g^+_5,\Lambda^-_{(1)\,1},\underline{\phi^{(14)}_{I}})\ , \tag{51}$$

with $I=(2,3)$, and $\lambda_I=(p_2+p_3)\cdot\tilde\lambda_2=p_3\cdot\tilde\lambda_2$.

1. The first contribution, Eq. (49), is

$$\frac{\langle 1\ 5\rangle[2\ 5]\langle 1\ 2\rangle}{\langle 5\ 1\rangle[2\ 1]\langle 5\ 1\rangle}\cdot\frac{1}{\langle 3\ 4\rangle[3\ 4]}\cdot\langle 3\ 4\rangle\ =\ \frac{\langle 1\ 2\rangle}{\langle 1\ 5\rangle}\frac{[2\ 5]}{[2\ 1][3\ 4]}\ . \tag{52}$$

2. The second contribution (50) gives

$$\langle 1\ 2\rangle\cdot\frac{1}{\langle 1\ 2\rangle[1\ 2]}\cdot\frac{\langle 4\ 1\rangle[2\ 1]\langle 3\ 4\rangle}{\langle 4\ 5\rangle\langle 5\ 1\rangle[2\ 1]}\ =\ \frac{\langle 3\ 4\rangle\langle 4\ 1\rangle}{\langle 4\ 5\rangle\langle 5\ 1\rangle[1\ 2]}\ . \tag{53}$$

3. The third contribution (51), is

$$\langle 2\ 3\rangle\cdot\frac{1}{\langle 2\ 3\rangle[2\ 3]}\cdot\frac{\langle 1\ 4\rangle^2}{\langle 4\ 5\rangle\langle 5\ 1\rangle}\ =\ \frac{\langle 1\ 4\rangle^2}{\langle 4\ 5\rangle\langle 5\ 1\rangle[2\ 3]}\ . \tag{54}$$

We add up the three contributions (52), (53), (54) and using the momentum conservation identities obtain

$$A_5^{\mathcal{N}=4}(\Lambda^-_{(1)\,1},\Lambda^-_{(2)\,2},\Lambda^-_{(3)\,3},\Lambda^-_{(4)\,4},g^+_5)=\ -\ \frac{[2\ 5][3\ 5]}{[1\ 2][2\ 3][3\ 4]}\ . \tag{55}$$

which is again the correct answer for this amplitude, as can be easily seen from taking the complex conjugate of the corresponding analytic expression.

7. NMHV (- - -) Amplitudes with Two Fermions

In this and the following section we restrict to $\mathcal{N}\le 1$ theory. There is only one type of fermions, $\Lambda^1=\Lambda$. We start with the case of one fermion-antifermion pair, Λ^-, Λ^+, and an arbitrary number of gluons, g. The amplitude has schematic form, $A_n(\Lambda^-_{m_1},g^-_{m_2},g^-_{m_3},\Lambda^+_k)$, and without loss of generality we can have $m_1<m_2<m_3$. With these conventions, there are three different classes of amplitudes depending on the position of the Λ^+_k fermion relative to m_1,m_2,m_3:

$$A_n(\Lambda^-_{m_1},g^-_{m_2},g^-_{m_3},\Lambda^+_k)\ , \tag{56a}$$

$$A_n(\Lambda^-_{m_1},g^-_{m_2},\Lambda^+_k,g^-_{m_3})\ , \tag{56b}$$

$$A_n(\Lambda^-_{m_1},\Lambda^+_k,g^-_{m_2},g^-_{m_3})\ . \tag{56c}$$

Each of these three amplitudes receives contributions from different types of scalar diagrams in the CSW approach. In all of these scalar diagrams

there are precisely two MHV vertices connected to each other by a single scalar propagator [1]. We will always arrange these diagrams in such a way that the MHV vertex on the left has positive helicity on the internal line, and the right vertex has a negative helicity. Then, there are three choices one can make [9] for the pair of negative helicity particles to enter external lines of the left vertex, (m_1, m_2), (m_2, m_3), or (m_3, m_1). In addition to this, each diagram in $\mathcal{N} \leq 1$ theory corresponds to either a gluon exchange, or a fermion exchange.

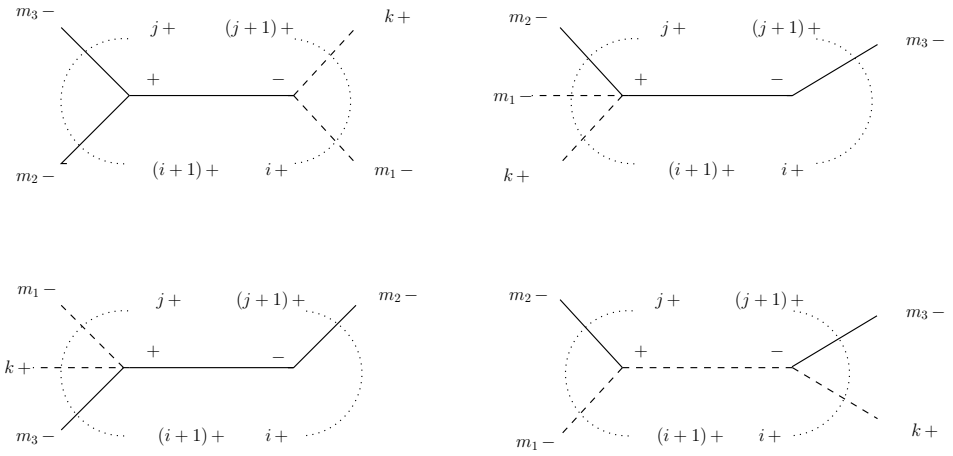

Figure 1. Diagrams with MHV vertices contributing to the amplitude $A_n(\Lambda^-_{m_1}, g^-_{m_2}, g^-_{m_3}, \Lambda^+_k)$. Fermions, Λ^+ and Λ^-, are represented by dashed lines and negative helicity gluons, g^-, by solid lines. Positive helicity gluons g^+ emitted from each vertex are indicated by dotted semicircles with labels showing the bounding g^+ lines in each MHV vertex.

The diagrams contributing to the first process (56a) are drawn in Figure 1. There are three gluon exchange diagrams for all three partitions (m_2, m_3), (m_1, m_2), (m_3, m_1), and there is one fermion exchange diagram for the partition (m_1, m_2).

It is straightforward, using the expressions for the MHV vertices (13),(14), to write down an analytic expression for the first diagram of Figure 1,

$$A_n^{(1)} = \frac{1}{\prod_{l=1}^n \langle l\ l+1\rangle} \sum_{i=m_1}^{m_2-1} \sum_{j=m_3}^{k-1} \frac{-\langle (i+1,j)\ m_1\rangle^3\ \langle (i+1,j)\ k\rangle}{\langle i\ (i+1,j)\rangle \langle (i+1,j)\ j+1\rangle} \times \frac{\langle i\ i+1\rangle \langle j\ j+1\rangle}{q^2_{i+1,j}} \frac{\langle m_2\ m_3\rangle^4}{\langle (j+1,i)\ i+1\rangle \langle j\ (j+1,i)\rangle} \,. \tag{57}$$

This expression is a direct rendering of the 'Feynman rules' for the scalar graph method [1, 6], followed by factoring out the overall factor of $(\prod_{l=1}^{n} \langle l\ l+1\rangle)^{-1}$. The objects $(i+1,j)$ and $(j+1,i)$ appearing on the right hand side of (57) denote the spinors $\lambda_{i+1,j}$ and $\lambda_{j+1,i}$ corresponding to the off-shell momentum $q_{i+1,j}$

$$\begin{aligned} &q_{i+1,j} \equiv\ p_{i+1} + p_{i+2} + \ldots + p_j\ ,\ q_{j+1,i} \equiv\ p_{j+1} + p_{j+2} + \ldots + p_i\ , \\ &q_{i+1,j} + q_{j+1,i} =\ 0\,, \\ &\lambda_{i+1,j\,a} \equiv\ q_{i+1,j\,a\dot{a}}\,\xi^{\dot{a}}_{\rm Ref} =\ -\lambda_{j+1,i\,a}\ , \end{aligned} \tag{58}$$

where $\xi^{\dot{a}}_{\rm Ref}$ is the reference (dotted) spinor [1] as in Eq. (16). All other spinors λ_i are on-shell and $\langle i\ (j,k)\rangle$ is an abbreviation for a spinor product $\langle \lambda_i, \lambda_{jk}\rangle$.

Having the freedom to choose any reference spinor we will always choose it to be the spinor of the fermion Λ^-. In this section, this is the spinor of $\Lambda^-_{m_1}$,

$$\xi^{\dot{a}}_{\rm Ref} =\ \tilde{\lambda}^{\dot{a}}_{m_1}\ . \tag{59}$$

We can now re-write

$$\begin{aligned} &\langle i\ (i+1,j)\rangle\langle (i+1,j)\ j+1\rangle\langle (j+1,i)\ i+1\rangle\langle j\ (j+1,i)\rangle \\ &= \langle i^-|\not{q}_{i+1,j}|m_1^-\rangle\langle j+1^-|\not{q}_{i+1,j}|m_1^-\rangle\langle i+1^-|\not{q}_{i+1,j}|m_1^-\rangle\langle j^-|\not{q}_{i+1,j}|m_1^-\rangle\ , \end{aligned} \tag{60}$$

and define a universal combination,

$$\begin{aligned} D = \langle i^-|\not{q}_{i+1,j}|m_1^-\rangle\langle j+1^-|\not{q}_{i+1,j}|m_1^-\rangle\langle i+1^-|\not{q}_{i+1,j}|m_1^-\rangle\langle j^-|\not{q}_{i+1,j}|m_1^-\rangle \\ \times \frac{q^2_{i+1,j}}{\langle i\ i+1\rangle\langle j\ j+1\rangle}\,. \end{aligned} \tag{61}$$

Note that here we introduced the standard Lorentz-invariant matrix element $\langle i^-|\not{p}_{\ k}|j^-\rangle = i^a\, p_{k\ a\dot{a}}\, j^{\dot{a}}$, which in terms of the spinor products is

$$\langle i^-|\not{p}_{\ k}|j^-\rangle =\ \langle i^-|^a\ |k^+\rangle_a\ \langle k^+|_{\dot{a}}\ |j^-\rangle^{\dot{a}} =\ -\langle i\ k\rangle\,[k\ j] =\ \langle i\ k\rangle\,[j\ k]\ . \tag{62}$$

The expression for $A_n^{(1)}$ now becomes

$$A_n^{(1)} = \frac{-1}{\prod_{l=1}^{n}\langle l\ l+1\rangle} \sum_{i=m_1}^{m_2-1}\sum_{j=m_3}^{k-1} \frac{\langle m_1^-|\not{q}_{i+1,j}|m_1^-\rangle^3\langle k^-|\not{q}_{i+1,j}|m_1^-\rangle\langle m_2\ m_3\rangle^4}{D}\ . \tag{63}$$

For the second diagram of Figure 1, we have

$$A_n^{(2)} = \frac{-1}{\prod_{l=1}^n \langle l\ l+1\rangle} \sum_{i=m_3}^{k-1} \sum_{j=m_2}^{m_3-1} \frac{\langle m_3^- | \not{q}_{i+1,j} | m_1^- \rangle^4 \langle m_2\ m_1\rangle^3 \langle m_2\ k\rangle}{D} \ . \quad (64)$$

The MHV vertex on the right in the second diagram in Figure 1 can collapse to a 2-leg vertex. This occurs when $i = m_3$ and $j+1 = m_3$. This vertex is identically zero, since $q_{j+1,i} = p_{m_3} = -q_{i+1,j}$, and $\langle m_3\ m_3\rangle = 0$. Similar considerations apply in (65), (68), (68), (69), (69), (71) and (72).

Expressions corresponding to the third and fourth diagrams in Figure 1 are

$$A_n^{(3)} = \frac{-1}{\prod_{l=1}^n \langle l\ l+1\rangle} \sum_{i=m_2}^{m_3-1} \sum_{j=m_1}^{m_2-1} \frac{\langle m_2^- | \not{q}_{i+1,j} | m_1^- \rangle^4 \langle m_3\ m_1\rangle^3 \langle m_3\ k\rangle}{D} \ , \quad (65)$$

$$A_n^{(4)} = \frac{-1}{\prod_{l=1}^n \langle l\ l+1\rangle} \times \sum_{i=k}^{n+m_1-1} \sum_{j=m_2}^{m_3-1} \frac{\langle m_3^- | \not{q}_{i+1,j} | m_1^- \rangle^3 \langle m_2^- | \not{q}_{i+1,j} | m_1^- \rangle \langle m_2\ m_1\rangle^3 \langle m_3\ k\rangle}{D} \ . \quad (66)$$

Note that the first sum in (66), $\sum_{i=k}^{n+m_1-1}$, is understood to run in cyclic order, for example $\sum_{i=4}^{3} = \sum_{i=4,\ldots,n,1,2,3}$. The same comment will also apply to similar sums in Eqs. (68), (68), (69), (69) below.

The total amplitude is the sum of (63), (64), (65) and (66),

$$A_n(\Lambda_{m_1}^-, g_{m_2}^-, g_{m_3}^-, \Lambda_k^+) = \sum_{i=1}^{4} A_n^{(i)} \ . \quad (67)$$

There are three sources of zeroes in the denominator combination D defined in (61). First, there are genuine zeroes in, for example, $\langle i^- | \not{q}_{i+1,j} | m_1^- \rangle$ when $q_{i+1,j}$ is proportional to p_i. This occurs when $j = i-1$. Such terms are always associated with two-leg vertices as discussed above and produce zeroes in the numerator. In fact, the number of zeroes in the numerator always exceeds the number of zeroes in the denominator and this contribution vanishes. Second, there are zeroes associated with three-point vertices when, for example, $i = m_2$ and $q_{i+1,j} = p_{m_2} + p_{m_1}$ so that $\langle m_2^- | \not{n}_1 + \not{n}_2 | m_1^- \rangle = 0$. As discussed in Sec. 2, there is always a compensating factor in the numerator. Such terms give a finite contribution (see (20)). Third, there are accidental zeroes when $q_{i+1,j}$ happens to be a linear combination of p_i and p_{m_1}. For general phase space points this is not the case. However, at certain phase space points, the Gram determinant of p_i, p_{m_1} and $q_{i+1,j}$ does vanish. This

produces an apparent singularity in individual terms in (63)–(66) which cancels when all contributions are taken into account. This cancellation can be achieved numerically or straightforwardly eliminated using standard spinor techniques [9].

For the special case of coincident negative helicities, $m_1 = 1$, $m_2 = 2$, $m_3 = 3$, the double sums in Eqs. (63)–(66) collapse to single sums. Furthermore, we see that the contribution from (65) vanishes due to momentum conservation, $q_{2,1} = 0$. The remaining three terms agree with the result presented in Eq. (3.6) of Ref. [6].

We now consider the second amplitude, Eq. (56b). The scalar graph diagrams are shown in Figure 2. There is a fermion exchange and a gluon exchange diagram for two of the line assignments, (m_1, m_2), and (m_3, m_1), and none for the remaining assignment (m_2, m_3). These four diagrams result in:

$$
\begin{aligned}
A_n^{(1)'} &= \frac{1}{\prod_{l=1}^{n} \langle l\ l+1\rangle} \\
&\quad \times \sum_{i=m_3}^{n+m_1-1} \sum_{j=m_2}^{k-1} \frac{\langle m_3^- | \not{q}_{i+1,j} | m_1^- \rangle^3 \langle m_2^- | \not{q}_{i+1,j} | m_1^- \rangle \langle m_2\ m_1\rangle^3 \langle m_3\ k\rangle}{D}\,, \\
A_n^{(2)'} &= \frac{1}{\prod_{l=1}^{n} \langle l\ l+1\rangle} \sum_{i=m_2}^{k-1} \sum_{j=m_1}^{m_2-1} \frac{\langle m_2^- | \not{q}_{i+1,j} | m_1^- \rangle^4 \langle m_3\ m_1\rangle^3 \langle m_3\ k\rangle}{D}\,, \\
A_n^{(3)'} &= \frac{1}{\prod_{l=1}^{n} \langle l\ l+1\rangle} \\
&\quad \times \sum_{i=k}^{m_3-1} \sum_{j=m_1}^{m_2-1} \frac{\langle m_2^- | \not{q}_{i+1,j} | m_1^- \rangle^3 \langle m_3^- | \not{q}_{i+1,j} | m_1^- \rangle \langle m_3\ m_1\rangle^3 \langle m_2\ k\rangle}{D}\,, \\
A_n^{(4)'} &= \frac{-1}{\prod_{l=1}^{n} \langle l\ l+1\rangle} \sum_{i=m_3}^{n+m_1-1} \sum_{j=k}^{m_3-1} \frac{\langle m_3^- | \not{q}_{i+1,j} | m_1^- \rangle^4 \langle m_2\ m_1\rangle^3 \langle m_2\ k\rangle}{D}\,,
\end{aligned}
$$

and the final answer for (56b) is,

$$
A_n(\Lambda_{m_1}^-, g_{m_2}^-, \Lambda_k^+, g_{m_3}^-) = \sum_{i=1}^{4} A_n^{(i)'}\ . \tag{68}
$$

Finally, we give the result for (56c). The corresponding diagrams are drawn in Figure 3. We find

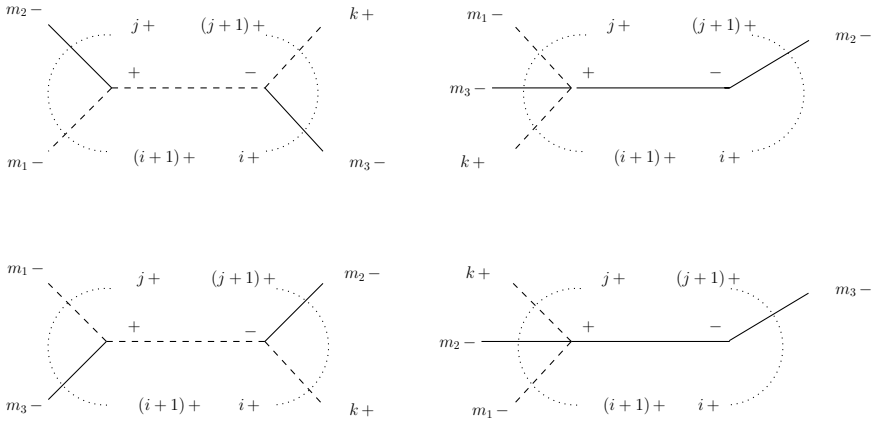

Figure 2. Diagrams with MHV vertices contributing to the amplitude $A_n(\Lambda^-_{m_1}, g^-_{m_2}, \Lambda^+_k, g^-_{m_3})$.

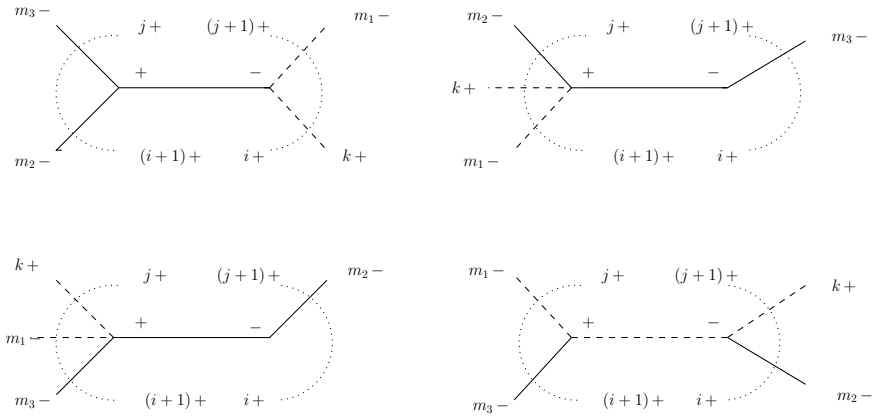

Figure 3. Diagrams with MHV vertices contributing to the amplitude $A_n(\Lambda^-_{m_1}, \Lambda^+_k, g^-_{m_2}, g^-_{m_3})$.

$$A_n^{(1)''} = \frac{1}{\prod_{l=1}^n \langle l\ l{+}1\rangle} \sum_{i=k}^{m_2-1} \sum_{j=m_3}^{n+m_1-1} \frac{\langle m_1^- | \not{q}_{i+1,j} | m_1^- \rangle^3 \langle k^- | \not{q}_{i+1,j} | m_1^- \rangle \langle m_2\ m_3\rangle^4}{D}\ ,$$

$$A_n^{(2)''} = \frac{1}{\prod_{l=1}^n \langle l\ l{+}1\rangle} \sum_{i=m_3}^{n+m_1-1} \sum_{j=m_2}^{m_3-1} \frac{\langle m_3^- | \not{q}_{i+1,j} | m_1^- \rangle^4 \langle m_2\ m_1\rangle^3 \langle m_2\ k\rangle}{D}\ ,$$

$$A_n^{(3)''} = \frac{1}{\prod_{l=1}^n \langle l\ l{+}1\rangle} \sum_{i=m_2}^{m_3-1} \sum_{j=k}^{m_2-1} \frac{\langle m_2^- | \not{q}_{i+1,j} | m_1^- \rangle^4 \langle m_3\ m_1\rangle^3 \langle m_3\ k\rangle}{D}\ ,$$

$$A_n^{(4)''} = \frac{-1}{\prod_{l=1}^n \langle l\ l{+}1\rangle} \sum_{i=m_2}^{m_3-1} \sum_{j=m_1}^{k-1} \frac{\langle m_2^- | \not{q}_{i+1,j} | m_1^- \rangle^3 \langle m_3^- | \not{q}_{i+1,j} | m_1^- \rangle \langle m_3\ m_1\rangle^3 \langle m_2\ k\rangle}{D}\ .$$

As before, the full amplitude is given by the sum of contributions,

$$A_n(\Lambda^-_{m_1},\Lambda^+_k,g^-_{m_2},g^-_{m_3}) = \sum_{i=1}^{4} A_n^{(i)\prime\prime} \ . \tag{69}$$

8. NMHV (- - -) Amplitudes with Four Fermions

We now consider the amplitudes with 2 fermion-antifermion lines. In what follows, without loss of generality we will choose the negative helicity gluon to be the first particle. With this convention, we can write the six inequivalent amplitudes as:

$$A_n(g^-_1,\Lambda^-_{m_2},\Lambda^-_{m_3},\Lambda^+_{m_p},\Lambda^+_{m_q}) \ , \tag{70a}$$

$$A_n(g^-_1,\Lambda^-_{m_2},\Lambda^+_{m_p},\Lambda^-_{m_3},\Lambda^+_{m_q}) \ , \tag{70b}$$

$$A_n(g^-_1,\Lambda^-_{m_2},\Lambda^+_{m_p},\Lambda^+_{m_q},\Lambda^-_{m_3}) \ , \tag{70c}$$

$$A_n(g^-_1,\Lambda^+_{m_p},\Lambda^-_{m_2},\Lambda^-_{m_3},\Lambda^+_{m_q}) \ , \tag{70d}$$

$$A_n(g^-_1,\Lambda^+_{m_p},\Lambda^-_{m_2},\Lambda^+_{m_q},\Lambda^-_{m_3}) \ , \tag{70e}$$

$$A_n(g^-_1,\Lambda^+_{m_p},\Lambda^+_{m_q},\Lambda^-_{m_2},\Lambda^-_{m_3}) \ . \tag{70f}$$

The calculation of the amplitudes of (70a)-(70f) is straightforward [10]. The diagrams contributing to the first process are shown in Figure 4. It should be noted that not all the amplitudes in (70a)-(70f) receive contributions from the same number of diagrams. For example, there are four diagrams for the process of (70a) while there are six for that of (70b). In order to avoid vanishing denominators, one can choose the reference spinor to be $\tilde{\eta} = \tilde{\lambda}_{m_2}$. With this choice the result can be written as:

$$\tilde{A}_n^{(1)} = \frac{1}{\prod_{l=1}^n \langle l\ l+1\rangle} \sum_{i=p}^{q-1}\sum_{j=m_2}^{m_3-1} \frac{\langle m_3^-|\not{q}_{i+1,j}|m_2^-\rangle^3\langle p^-|\not{q}_{i+1,j}|m_2^-\rangle\langle 1\ m_2\rangle^3\langle 1\ q\rangle}{D} \ ,$$

$$\tilde{A}_n^{(2)} = \frac{-1}{\prod_{l=1}^n \langle l\ l+1\rangle} \sum_{i=1}^{m_2-1}\sum_{j=q}^{n} \frac{\langle 1^-|\not{q}_{i+1,j}|m_2^-\rangle^4\langle m_2\ m_3\rangle^3\langle p\ q\rangle}{D} \ ,$$

$$\tilde{A}_n^{(3)} = \frac{1}{\prod_{l=1}^n \langle l\ l+1\rangle} \sum_{i=1}^{m_2-1}\sum_{j=p}^{q-1} \frac{\langle 1^-|\not{q}_{i+1,j}|m_2^-\rangle^3\langle p^-|\not{q}_{i+1,j}|m_2^-\rangle\langle m2\ m_3\rangle^3\langle 1\ q\rangle}{D} \ ,$$

$$\tilde{A}_n^{(4)} = \frac{-1}{\prod_{l=1}^n \langle l\ l+1\rangle} \sum_{i=q}^{n}\sum_{j=m_2}^{m_3-1} \frac{\langle m_3^-|\not{q}_{i+1,j}|m_2^-\rangle^3\langle 1^-|\not{q}_{i+1,j}|m_2^-\rangle\langle 1\ m_2\rangle^3\langle p\ q\rangle}{D} \ .$$

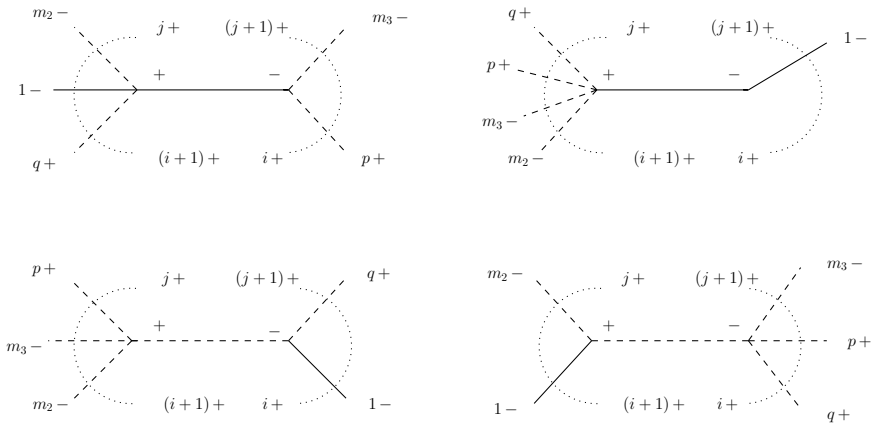

Figure 4. Tree diagrams with MHV vertices contributing to the four fermion amplitude $A_n(g_1^-, \Lambda_{m_2}^-, \Lambda_{m_3}^-, \Lambda_{m_p}^+, \Lambda_{m_q}^+)$.

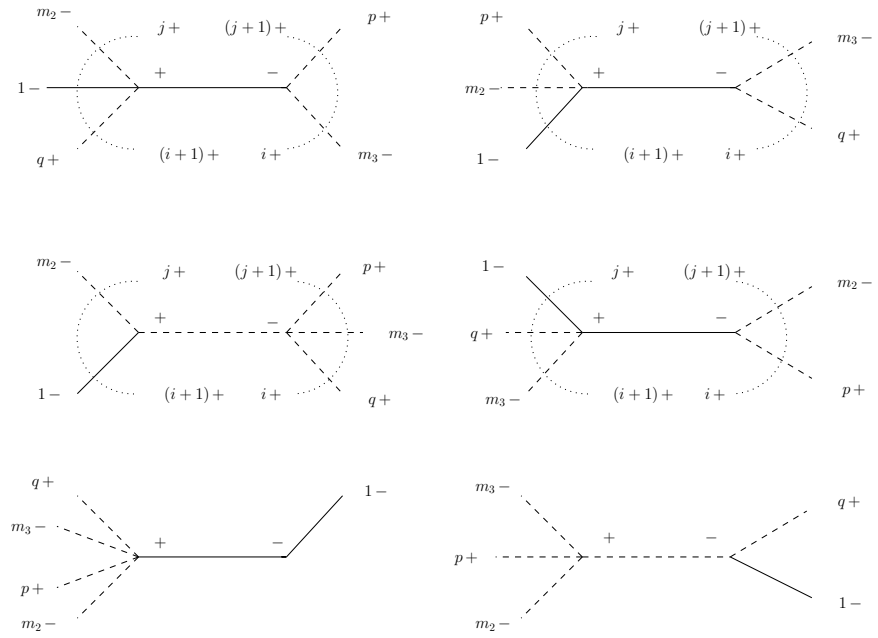

Figure 5. Tree diagrams with MHV vertices contributing to the four fermion amplitude $A_n(g_1^-, \Lambda_{m_2}^-, \Lambda_{m_p}^+, \Lambda_{m_3}^-, \Lambda_{m_q}^+)$.

As before the final result is the sum

$$A_n(g_1^-, \Lambda_{m_2}^-, \Lambda_{m_3}^-, \Lambda_{m_p}^+, \Lambda_{m_q}^+) = \sum_{i=1}^{4} \tilde{A}_n^{(i)} \ . \tag{71}$$

Once again, for the case of coincident negative helicities, $m_2 = 2$, $m_3 = 3$, the double sums collapse to single summations and we recover the results given in Ref. [6]. As a last example we write down the expression for the amplitude of (70b). The corresponding diagrams are shown in Figure 5. We find,

$$\tilde{A}_n^{(1)'} = \frac{-1}{\prod_{l=1}^n \langle l\ l{+}1\rangle} \sum_{i=m_3}^{q-1} \sum_{j=m_2}^{p-1} \frac{\langle m_3^- | \not{q}_{i+1,j} | m_2^- \rangle^3 \langle p^- | \not{q}_{i+1,j} | m_2^- \rangle \langle 1\ m_2\rangle^3 \langle 1\ q\rangle}{D},$$

$$\tilde{A}_n^{(2)'} = \frac{1}{\prod_{l=1}^n \langle l\ l{+}1\rangle} \sum_{i=q}^{n} \sum_{j=p}^{m_3-1} \frac{\langle m_3^- | \not{q}_{i+1,j} | m_2^- \rangle^3 \langle q^- | \not{q}_{i+1,j} | m_2^- \rangle \langle 1\ m_2\rangle^3 \langle 1\ p\rangle}{D},$$

$$\tilde{A}_n^{(3)'} = \frac{1}{\prod_{l=1}^n \langle l\ l{+}1\rangle} \sum_{i=q}^{n} \sum_{j=m_2}^{p-1} \frac{\langle m_3^- | \not{q}_{i+1,j} | m_2^- \rangle^3 \langle 1^- | \not{q}_{i+1,j} | m_2^- \rangle \langle 1\ m_2\rangle^3 \langle p\ q\rangle}{D},$$

$$\tilde{A}_n^{(4)'} = \frac{1}{\prod_{l=1}^n \langle l\ l{+}1\rangle} \sum_{i=p}^{m_3-1} \sum_{j=1}^{m_2-1} \frac{\langle m_2^- | \not{q}_{i+1,j} | m_2^- \rangle^3 \langle p^- | \not{q}_{i+1,j} | m_2^- \rangle \langle 1\ m_3\rangle^3 \langle 1\ q\rangle}{D},$$

$$\tilde{A}_n^{(5)'} = \frac{1}{\prod_{l=1}^n \langle l\ l{+}1\rangle} \sum_{i=1}^{m_2-1} \sum_{j=q}^{n} \frac{\langle 1^- | \not{q}_{i+1,j} | m_2^- \rangle^4 \langle m_2\ m_3\rangle^3 \langle p\ q\rangle}{D},$$

$$\tilde{A}_n^{(6)'} = \frac{-1}{\prod_{l=1}^n \langle l\ l{+}1\rangle} \sum_{i=1}^{m_2-1} \sum_{j=m_3}^{q-1} \frac{\langle 1^- | \not{q}_{i+1,j} | m_2^- \rangle^3 \langle p^- | \not{q}_{i+1,j} | m_2^- \rangle \langle m_2\ m_3\rangle^3 \langle 1\ q\rangle}{D}.$$

And the full amplitude is

$$A_n(g_1^-, \Lambda_{m_2}^-, \Lambda_{m_p}^+, \Lambda_{m_3}^-, \Lambda_{m_q}^+) = \sum_{i=1}^{6} \tilde{A}_n^{(i)'}\ . \tag{72}$$

We close this section by listing the inequivalent NMHV amplitudes with three fermion–antifermion pairs. There are ten such amplitudes since choosing the first particle to be a negative helicity fermion we are left with five fermions (two of which have negative helicity and three positive) which should be distributed in all possible ways among themselves, and, in addition there are $(n-6)$ positive helicity gluons. Thus the number of different possible ways is 5!. However, the order of the particles of the same helicity is immaterial (since one can always choose $m_2 \leq m_3$ and $m_p \leq m_q \leq m_r$). This means that we have to divide 5! by 3! (for the positive helicity fermions) and by 2! (for the negative helicity fermions.) Thus there are ten different

fermion amplitudes. These are listed below:

$$
\begin{aligned}
&A_n(\Lambda_1^-,\Lambda_{m_2}^-,\Lambda_{m_3}^-,\Lambda_{m_p}^+,\Lambda_{m_q}^+,\Lambda_{m_r}^+)\ , \quad A_n(\Lambda_1^-,\Lambda_{m_2}^-,\Lambda_{m_p}^+,\Lambda_{m_3}^-,\Lambda_{m_q}^+,\Lambda_{m_r}^+)\ ,\\
&A_n(\Lambda_1^-,\Lambda_{m_2}^-,\Lambda_{m_p}^+,\Lambda_{m_q}^+,\Lambda_{m_3}^-,\Lambda_{m_r}^+)\ , \quad A_n(\Lambda_1^-,\Lambda_{m_p}^+,\Lambda_{m_2}^-,\Lambda_{m_3}^-,\Lambda_{m_q}^+,\Lambda_{m_r}^+)\ ,\\
&A_n(\Lambda_1^-,\Lambda_{m_p}^+,\Lambda_{m_2}^-,\Lambda_{m_q}^+,\Lambda_{m_3}^-,\Lambda_{m_r}^+)\ , \quad A_n(\Lambda_1^-,\Lambda_{m_p}^+,\Lambda_{m_q}^+,\Lambda_{m_2}^-,\Lambda_{m_3}^-,\Lambda_{m_r}^+)\ ,\\
&A_n(\Lambda_1^-,\Lambda_{m_p}^+,\Lambda_{m_q}^+,\Lambda_{m_r}^+,\Lambda_{m_2}^-,\Lambda_{m_3}^-)\ , \quad A_n(\Lambda_1^-,\Lambda_{m_p}^+,\Lambda_{m_q}^+,\Lambda_{m_2}^-,\Lambda_{m_r}^+,\Lambda_{m_3}^-)\ ,\\
&A_n(\Lambda_1^-,\Lambda_{m_p}^+,\Lambda_{m_2}^-,\Lambda_{m_q}^+,\Lambda_{m_r}^+,\Lambda_{m_3}^-)\ , \quad A_n(\Lambda_1^-,\Lambda_{m_2}^-,\Lambda_{m_p}^+,\Lambda_{m_q}^+,\Lambda_{m_r}^+,\Lambda_{m_3}^-)\ .
\end{aligned}
\tag{73}
$$

These amplitudes also present no difficulty, and they can be evaluated in the same manner as before.

9. Two analytic supervertices

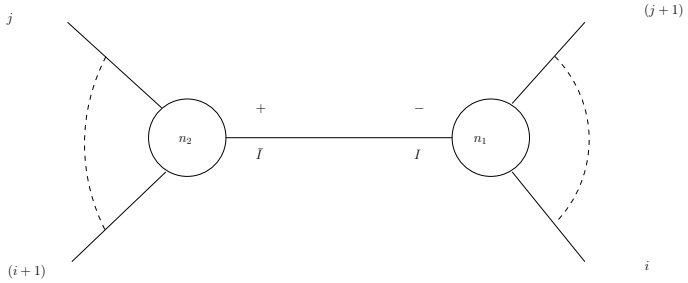

Figure 6. Tree diagram with two analytic supervertices.

We now consider a diagram with two analytic supervertices (28) connected to one another by a single scalar propagator. The diagram is depicted in Figure 6. We follow the same conventions as in the previous sections, and the left vertex has a positive helicity on the internal line $\bar{I}$, while the right vertex has a negative helicity on the internal line I. The labelling of the external lines in Figure 6 is also consistent with our conventions. The right vertex has n_1 lines, and the left one has n_2 lines in total, such that resulting amplitude A_n has $n = n_1 + n_2 - 2$ external lines. Suppressing summations over the distribution of n_1 and n_2 between the two vertices, we can write down an expression for the corresponding amplitude which follows immediately from (28) and Figure 6,

$$
\begin{aligned}
A_n = &\frac{1}{\prod_{l=1}^n \langle l\ l+1\rangle}\ \frac{1}{q_I^2}\ \frac{\langle j\ j+1\rangle\langle i\ i+1\rangle}{\langle j\ \bar{I}\rangle\langle \bar{I}\ i+1\rangle\langle i\ I\rangle\langle I\ j+1\rangle}\\
&\times \int \prod_{A=1}^4 d\eta_I^A\ \delta^{(8)}\Big(\lambda_{\bar{I}a}\eta_I^A + \sum_{l_2\neq\bar{I}}^{n_2}\lambda_{l_2 a}\eta_{l_2}^A\Big)\ \delta^{(8)}\Big(\lambda_{Ia}\eta_I^A + \sum_{l_1\neq I}^{n_1}\lambda_{l_1 a}\eta_{l_1}^A\Big)\ .
\end{aligned}
\tag{74}
$$

The two delta-functions in (74) come from the two vertices (28). The summations in the delta-function arguments run over the $n_1 - 1$ external lines for right vertex, and $n_2 - 1$ external lines for the left one. The integration over $d^4\eta_I$ arises in (74) for the following reason. Two separate (unconnected) vertices in Figure 6 would have $n_1 + n_2$ lines and, hence, $n_1 + n_2$ different η's (and λ's). However the I and the $\bar{I}$ lines are connected by the propagator, and there must be only $n = n_1 + n_2 - 2$ η-variables left. This is achieved in (74) by setting

$$\eta_{\bar{I}}^A = \eta_I^A \ , \tag{75}$$

and integrating over $d^4\eta_I$. The off-shell continuation of the internal spinors is defined as before,

$$\lambda_{Ia} = \sum_{l_1 \neq I}^{n_1} p_{l_1 \, a\dot{a}} \ \xi^{\dot{a}}_{\rm Ref} = -\lambda_{\bar{I}a} \ . \tag{76}$$

We now integrate out four η_I's which is made simple by rearranging the arguments of the delta-functions via $\int \delta(f_2)\delta(f_1) = \int \delta(f_1 + f_2)\delta(f_1)$, and noticing that the sum of two arguments, $f_1 + f_2$, does not depend on η_I.

The final result is

$$A_n = \frac{1}{\prod_{l=1}^n \langle l \ l+1\rangle} \ \delta^{(8)}\Big(\sum_{i=1}^n \lambda_{ia}\eta_i^A\Big) \ \prod_{A=1}^4 \Big(\sum_{l_1 \neq I}^{n_1} \langle I \ l_1\rangle \eta_{l_1}^A\Big) \ \frac{1}{D} \ , \tag{77}$$

and D is the same as (61) used in Sections 3 and 4,

$$\frac{1}{D} \ = \ \frac{1}{q_I^2} \ \frac{\langle j \ j+1\rangle\langle i \ i+1\rangle}{\langle j \ I\rangle\langle I \ i+1\rangle\langle i \ I\rangle\langle I \ j+1\rangle} \ . \tag{78}$$

There are 12 η's in the superamplitude (77), and the coefficients of the Taylor expansion in η's give all the component amplitudes of degree-12.

10. One-Loop Results

The next logical step is to extend the formalism to the computation of loop graphs. The simplicity and elegant structure of tree level and also loop amplitudes in gauge theory was quantified in [4] by reinterpreting these amplitudes in terms of a topological string theory with twistor space as a target.

At present we do not know how to compute SYM loop amplitudes directly from string theory. It was noted in [22] that the currently known topological string models conjectured to be dual to $\mathcal{N} = 4$ SYM, at loop level describe

SYM coupled to conformal supergravity. No obvious way was found to decouple supergravitons circulating in the loops. Also, loop amplitudes in SYM directly in 4 spacetime dimensions suffer from infrared (IR) – soft and collinear – divergences. At tree level there are no integrations over loop momenta and IR divergences in the amplitudes can be avoided by selecting a non-exceptional set of external momenta (i.e the set with none of the external momenta being collinear or soft). Hence tree amplitudes can be made IR finite and it is meaningful to be calculating them directly in 4D without an explicit IR cutoff. Loop amplitudes, however, are always IR divergent and one cannot choose a set of external momenta which would make an on-shell loop amplitude finite in 4D. Any successful string computation of loop amplitudes in gauge theory will have to provide an infrared cutoff, i.e. a sort of dimensional regularization, but it is not entirely clear at present how this is encoded in the string with target space $CP^{3|4}$ [6].

Having said this, we expect that it is very likely that twistor space $CP^{3|4}$ will continue to play an important rôle for understanding amplitudes at loop level. The origins of the tree level CSW method [1] lay in the unexpected simplicity of tree-level SYM amplitudes in the helicity basis transformed to twistor space. Recently it was shown in [11] that when gauge theory amplitudes at 1-loop level are Fourier transformed to twistor space, their analytic structure again acquires geometric meaning. It is not known what kind of twistor string theory can generate this geometric structure.

Instead of appealing to string theory, it appears to be more productive (at present) to calculate loop amplitudes directly in SYM in scalar perturbation theory of CSW [1]. In order to compute 1-loop amplitudes with the CSW scalar graph method one can choose two different routes. The first is to use the unitarity approach of Bern, Dixon, Dunbar and Kosower [28] for sewing tree amplitudes to form loops. The CSW method [1] can be used here to efficiently calculate tree amplitudes [6, 9, 10], as reviewed in Sections 3, 7, 8, 9 above, and 1-loop amplitudes would be obtained from these trees by sewing them together and using the cut-constructibility method [28]. This is a promising direction for future study, which cannot fail to lead to new results. The second approach, is a direct calculation of loop diagrams in the CSW scalar graph perturbation theory. A priori, there is no proof that the original CSW approach should work beyond tree level. Moreover, the twistor space motivation (given in Section 2 of [11]) of the tree level CSW formalism [1], does not apply directly to loop amplitudes. Nevertheless, the success of the CSW method at tree level is encouraging enough to try to apply it at 1-loop level. The first such calculations were carried out very

recently by Brandhuber, Spence and Travaglini in [12].

The authors of [12] have calculated 1-loop MHV amplitudes in $\mathcal{N} = 4$ theory directly using the CSW scalar graph Feynman rules. This is done by taking off-shell and joining together two external lines from two different vertices in Figure 6, thus obtaining a 1-loop MHV diagram with two tree-level analytic supervertices. Carrying out the integration over the loop momentum and summing over all inequivalent 1-loop diagrams gives the final result for this amplitude. Remarkably, this result turns out to be in precise agreement with the earlier expression derived in [28], thus vindicating the CSW method at 1-loop level in the simplest case of $\mathcal{N} = 4$ theory and for MHV loop diagrams.

The calculation of [12] is facilitated by finding a particularly convenient representation for the integral over the loop momentum. An off-shell loop momentum L^μ can be represented as a linear combination of an on-shell momentum l^μ and a reference momentum $\xi^\mu_{\rm Ref}$ which is also on-shell [8, 9],

$$L^\mu \,=\, l^\mu \,+\, z\,\xi^\mu_{\rm Ref}\ , \quad l^2 \,=\, 0\ , \quad \xi^2_{\rm Ref} \,=\, 0\ , \tag{79}$$

where z is a real number,

$$z \,=\, \frac{L^2}{2(L\,\xi_{\rm Ref})}\ . \tag{80}$$

We now write the on-shell vectors l and $\xi_{\rm Ref}$ in terms of spinors as $l_{a\dot a} = l_a \tilde l_{\dot a}$ and $\xi^{\dot a a}_{\rm Ref} = \tilde\xi^{\dot a}_{\rm Ref}\xi^a_{\rm Ref}$, and find that

$$l_a \;=\; \frac{L_{a\dot a}\,\tilde\xi^{\dot a}_{\rm Ref}}{[\tilde l\ \tilde\xi_{\rm Ref}]} \;=>\; L_{a\dot a}\,\tilde\xi^{\dot a}_{\rm Ref}\ , \tag{81a}$$

$$\tilde l_{\dot a} \;=\; \frac{\xi^a_{\rm Ref}\,L_{a\dot a}}{\langle l\ \xi_{\rm Ref}\rangle} \;=>\; \xi^a_{\rm Ref}\,L_{a\dot a}\ . \tag{81b}$$

The denominators on the right hand sides of (81a) and (81b) are dropped because the final expressions for the amplitude are homogeneous in variables l and $\tilde l$.

Note that equation (81a) is identical to the off-shell continuation prescription (16) used so far. Hence the off-shell continuation of external legs for loop amplitudes is precisely the same as at tree level.

The integration over the loop momentum can now be represented in a particularly useful form [12] in terms of z and the on-shell spinors l, $\tilde l$,

$$\frac{d^4L}{L^2} \;=\; \frac{dz}{z}\,d\mu(l,\tilde l)\ , \tag{82}$$

where $d\mu(l,\tilde{l})$ is the Nair's measure [23],

$$d\mu(l,\tilde{l}) \;=\; \langle l\; dl\rangle\, d^2\tilde{l} \;-\; [\tilde{l}\; d\tilde{l}]\, d^2 l \;. \tag{83}$$

This representation of the integration measure over the loop momentum in terms of on-shell spinors and the variable z allows a straightforward evaluation of the loop integral in [12]. Another useful property [12] of Nair's measure $d\mu(l,\tilde{l})$ is that it is equal to the Lorentz-invariant space measure for a massless particle,

$$d\mu(l,\tilde{l}) \;\sim\; d^4 l\, \delta^{(+)}(l^2) \;. \tag{84}$$

This fact makes a remarkable connection between the direct evaluation of loop integrals and the unitarity approach of [28].

It will be very interesting to extend the results of [12] and to see if and how the CSW formalism will work in general settings, i.e. at 1-loop and beyond, for $\mathcal{N} \leq 4$ supersymmetry, and for non-MHV amplitudes.

11. Conclusions

We summarize by returning to the questions listed in the introduction.

First we consider tree level amplitudes.

(1) The CSW method works in pure gauge sector and in a supersymmetric theory. This was discussed in the introduction and it follows from considerations in Section 2.1 and calculations in Sections 3, 6 – 8.
(2) The method works in a generic supersymmetric gauge theory with $\mathcal{N} = 1, 2, 4$ supersymmetries. This follows from calculations in Section 6 and also from Sections 7 – 9.
(3) At tree level the method also works in $\mathcal{N}$=0 theory, such as QCD, and
(4) It works for finite number of colors, as explained in the Introduction and in Section 2.1
(5) The purpose of Sections 7, 8 and 3 and of [10] was to demonstrate that large classes of previously unknown tree amplitudes with gluons and fermions can now be calculated straightforwardly. No further helicity-spinor algebra is required to convert the results into a numerically usable form. In principle one could use the results presented here to write a numerical program for evaluating generic tree-level processes involving fermions and bosons.

At loop level:

(6) So far the calculations at 1-loop level were carried out only in $\mathcal{N} = 4$ theory. It is known [12] that the method works correctly in $\mathcal{N} = 4$

for MHV amplitudes and at 1-loop. Given this and the fact that the method was successful at tree level in general settings, it is likely that it will work for general supersymmetric theories at 1-loop level and for NMHV loop diagrams.

(7) There are known difficulties in applying the CSW method $\mathcal{N} = 0$ theories at 1-loop level, as outlined in Section 5.2 of [11]. At best, the original CSW method needs to be modified by adding additional off-shell 1-loop vertices as new building blocks.

(8) So far the calculations at loop level were performed in the planar limit. It is not known whether the method can be used to find non-planar contributions.

The list of things to do includes:

- Calculate NMHV 1-loop diagrams in $\mathcal{N} = 4$ theory.
- Calculate MHV (and NMHV) amplitudes in $\mathcal{N} = 1$ theory using either direct loop integrations or by sewing trees.
- Consider modifications of the method for nonsupersymmetric theories at loop level.
- Include masses.
- Find a twistor space interpretation of the 1-loop calculation in [12] and compare it with [11].
- Search for a string theory calculation of 1-loop amplitudes.
- Understand higher loops, at least in $\mathcal{N} = 4$ SYM.

Acknowledgments

This contribution is an extended version of my talk at 'Continuous Advances in QCD 2004' and it follows closely Refs. [6, 10]. I thank the organizers for an excellent conference and George Georgiou and Nigel Glover for an enjoyable collaboration and for greatly contributing to my understanding of these topics. I am grateful to Zvi Bern, Arnd Brandenburg, David Kosower, Misha Shifman, Andrei Smilga, Arkady Vainshtein and especially to Lance Dixon and Gabriele Travaglini for useful discussions and comments. This work is supported by a PPARC Senior Fellowship.

Dedicated to the memory of Ian Kogan.

References

1. F. Cachazo, P. Svrcek and E. Witten, *MHV vertices and tree amplitudes in gauge theory*, hep-th/0403047.
2. S. J. Parke and T. R. Taylor, Phys. Rev. Lett. **56**, 2459 (1986).
3. F. A. Berends and W. T. Giele, Nucl. Phys. B **306**, 759 (1988).
4. E. Witten, *Perturbative gauge theory as a string theory in twistor space*, hep-th/0312171.
5. C. J. Zhu, JHEP **0404**, 032 (2004) [hep-th/0403115].
6. G. Georgiou and V. V. Khoze, JHEP **0405**, 070 (2004) [hep-th/0404072].
7. J. B. Wu and C. J. Zhu, JHEP **0407**, 032 (2004) [hep-th/0406085].
8. I. Bena, Z. Bern and D. A. Kosower, *Twistor-space recursive formulation of gauge theory amplitudes*, hep-th/0406133.
9. D. A. Kosower, *Next-to-maximal helicity violating amplitudes in gauge theory*, hep-th/0406175.
10. G. Georgiou, E. W. N. Glover and V. V. Khoze, JHEP **0407**, 048 (2004) [hep-th/0407027].
11. F. Cachazo, P. Svrcek and E. Witten, *Twistor space structure of one-loop amplitudes in gauge theory*, hep-th/0406177.
12. A. Brandhuber, B. Spence and G. Travaglini, *One-loop gauge theory amplitudes in $\mathcal{N} = 4$ super Yang–Mills from MHV vertices*, hep-th/0407214.
13. R. Roiban, M. Spradlin and A. Volovich, JHEP **0404**, 012 (2004) [hep-th/0402016].
14. R. Roiban, M. Spradlin and A. Volovich, *On the tree-level S-matrix of Yang–Mills theory*, hep-th/0403190.
15. N. Berkovits, *An alternative string theory in twistor space for $\mathcal{N} = 4$ super-Yang–Mills*, hep-th/0402045; N. Berkovits and L. Motl, JHEP **0404**, 056 (2004) [hep-th/0403187].
16. A. Neitzke and C. Vafa, *$\mathcal{N} = 2$ strings and the twistorial Calabi-Yau*, hep-th/0402128. N. Nekrasov, H. Ooguri and C. Vafa, *S-duality and topological strings*, hep-th/0403167.
17. E. Witten, *Parity invariance for strings in twistor space*, hep-th/0403199.
18. S. Gukov, L. Motl and A. Neitzke, *Equivalence of twistor prescriptions for super Yang–Mills*, hep-th/0404085.
19. W. Siegel, *Untwisting the twistor superstring*, hep-th/0404255.
20. S. Giombi, R. Ricci, D. Robles-Llana and D. Trancanelli, *A note on twistor gravity amplitudes*, hep-th/0405086.
21. A. D. Popov and C. Saemann, *On supertwistors, the Penrose-Ward transform and $\mathcal{N}$=4 super Yang–Mills theory*, hep-th/0405123.
22. N. Berkovits and E. Witten, *Conformal supergravity in twistor-string theory*, hep-th/0406051.
23. V. P. Nair, Phys. Lett. B **214**, 215 (1988).
24. M. L. Mangano and S. J. Parke, Phys. Rept. **200**, 301 (1991).
25. M. T. Grisaru, H. N. Pendleton and P. van Nieuwenhuizen, Phys. Rev. D **15**, 996 (1977); M. T. Grisaru and H. N. Pendleton, Nucl. Phys. B **124**, 81 (1977).
26. F. A. Berends, R. Kleiss, P. De Causmaecker, R. Gastmans and T. T. Wu, Phys. Lett. B **103**, 124 (1981); P. De Causmaecker, R. Gastmans, W. Troost and T. T. Wu, Nucl. Phys. B **206**, 53 (1982); R. Kleiss and W. J. Stirling, Nucl. Phys. B **262**, 235 (1985); J. F. Gunion and Z. Kunszt, Phys. Lett. B **161**, 333 (1985).
27. L. J. Dixon, *Calculating scattering amplitudes efficiently*, hep-ph/9601359.
28. Z. Bern, L. J. Dixon, D. C. Dunbar and D. A. Kosower, Nucl. Phys. B **425**, 217 (1994) [hep-ph/9403226]; *ibid* **435**, 59 (1995) [hep-ph/9409265]; Z. Bern, L. J. Dixon and D. A. Kosower, Nucl. Phys. Proc. Suppl. **51C**, 243 (1996) [hep-ph/9606378].